Group 4 Metal Complexes of Fluorous (Di)Alkoxide-(Di)Imino Ligands: Synthesis, Structure, Olefin Polymerization Catalysis, and Decomposition Pathways

Nicolas Marquet,[†] Evgueni Kirillov,[†] Thierry Roisnel,[†] Abbas Razavi,[#] and Jean-François Carpentier*,[†]

Catalysis and Organometallics, UMR 6226 Sciences Chimiques de Rennes, CNRS-University of Rennes 1, 35042 Rennes Cedex, France, and Total Petrochemicals Research, Zone Industrielle C, 7181 Feluy, Belgium

Received September 29, 2008

The coordination chemistry of fluorous (di)alkoxide-(di)imino ligands onto Ti(IV), Zr(IV), and Hf(IV) centers has been studied. The diimino-diol $[(CF_3)_2C(OH)CH_2C(Me){=}NCH_2-]_2$ ($\{ON^{Et}NO\}H_2$) reacts selectively with $Ti(OiPr)_2Cl_2$ and $Zr(CH_2Ph)_4$ to give the corresponding complexes $\{ON^{Et}NO\}TiCl_2$ (**1**) and $\{ON^{Et}NO\}Zr(CH_2Ph)_2$ (**2**), with concomitant alcohol and alkane elimination, respectively. Reactions of the imino-alcohols $(CF_3)_2C(OH)CH_2C(R^1){=}NR^2$ ($\{ON^{R1,R2}\}H$; R^1 = Me, Ph; R^2 = Ph, CH_2Ph) with $Ti(OiPr)_4$ and $M(CH_2Ph)_4$ (M = Zr, Hf) gave the corresponding complexes $Ti(OiPr)_2\{ON^{R1,R2}\}_2$ (**3a**,**b**) and $M(CH_2Ph)_2\{ON^{R1,R2}\}_2$ (M = Zr, **7a**,**b**,**c**; M = Hf, **8a**,**b**). Dibenzyl complexes **7** and **8** decompose above −30 °C by abstraction of a hydrogen from the methylene ligand backbone by a benzyl group to give $M(CH_2Ph)\{ON^{R1,R2}\}\{ON^{-R1,R2}\}$ complexes (M = Zr, **9a**−**c**; M = Hf, **10a**), in which a ligand unit ($\{ON^{-R1,R2}\}$) has been transformed to an α,β-unsaturated amido-alkoxy dianionic moiety. A slightly different process was observed for the pentafluorophenyl system $Zr(CH_2Ph)_2\{ON^{Me,ArF}\}_2$ (ArF = C_6F_5; **7d**), which ultimately yielded the benzyl-free complex $Zr\{ON^{Me,ArF}\}_2\{ON^{-Me,ArF}\}$ (**11**). Single-crystal X-ray diffraction studies revealed that complexes **1**, **3a**, **7a**, **7b**, **7d**, **8a**, and **11** are mononuclear in the solid state and adopt either C_1- or mostly C_{2v}-symmetric, distorted octahedral structures with planar coordination of the (di)imino-di(alkoxide) ligands. Multinuclear NMR studies indicate that most of the complexes adopt also a C_{2v}-symmetric structure in solution. Dichloride complexes $ZrCl_2\{ON^{R1,R2}\}_2$ (R^1 = Me, Ph; R^2 = Ph, C_6F_5; **12a**−**c**) were prepared by alkane elimination or salt metathesis. When activated by MAO, **3a**,**b** and **12a**−**c** lead to active but very unstable ethylene polymerization catalysts that afford very high molecular weight linear polyethylenes.

Introduction

Alkoxides are hard, electronegative π-donor ligands, which are quite attractive because they offer strong metal−oxygen bonds that are expected to stabilize complexes of a variety of electropositive metals.[1] Also, considerable variation in steric and electronic properties is possible thanks to the great variety of these ligands conveniently obtained from alcohols. These features have given alkoxides a key place in modern coordination chemistry of early transition and main group metals (groups 3−5, 13), in particular in the recent search for new-generation polymerization catalysts.[2] The synthetic chemistry of early transition metal complexes based on simple alkoxides proved to be, however, often complicated.[1] This is largely due to the high tendency of the relatively more basic alkoxide ligands (as compared to aryloxides) to act as bridging ligands, eventually resulting in (highly) agglomerated structures. The use of highly stable fluorous tertiary alcohol ligands affords an efficient strategy to overcome this difficulty. Introduction of electron-withdrawing CF_3 groups α to the alkoxide generates intra- and intermolecular repulsions, as well as a less basic alkoxide O-atom, and as a result, a less distinct bridging tendency is observed.[1,3] Following this line, we have described some bi- and tetradentate fluorous (di)alkoxide-(di)*amino* ligand systems that proved to be effective for preparing well-defined complexes of oxophilic metal centers such as Y(III), Zr(IV), and Al(III), and in turn developing valuable applications in polymerization catalysis.[4] Recently, we launched another class of bi- and tetradentate fluorous (di)alkoxide-(di)*imino* ligands,[5,6] which are

* Corresponding author. Fax: (+33)(0)223-236-939. E-mail: jean-francois.carpentier@univ-rennes1.fr.

[†] CNRS-University of Rennes 1.

[#] Total Petrochemicals Research.

(1) (a) Bradley, D. C.; Mehrotra, R. M.; Rothwell, I. P.; Singh, A. *Alkoxo and Aryloxo Derivatives of Metals*; Academic Press: London, 2001. (b) Mehrotra, R. M.; Singh, A. *Prog. Inorg. Chem.* **1997**, *46*, 239. (c) Hubert-Pfalzgraf, L. G. *Coord. Chem. Rev.* **1998**, *178*−*180*, 967. (d) Piers, W. E.; Emslie, D. J. H. *Coord. Chem. Rev.* **2002**, *131*, 233–234. (e) Edelmann, F. T.; Freckmann, D. M. M.; Schumann, H. *Chem. Rev.* **2002**, *102*, 1851.

(2) For reviews and leading articles on "post-metallocene" complexes of groups 3−5 and the lanthanides related to polymerization, see: (a) Britovsek, G. J. P.; Gibson, V. C.; Wass, D. F. *Angew. Chem., Int. Ed.* **1999**, *38*, 428. (b) Edelmann, F. T.; Freckmann, D. M. M.; Schumann, H. *Chem. Rev.* **2002**, *102*, 1851. (c) Gibson, V. C.; Spitzmesser, S. K. *Chem. Rev.* **2003**, *103*, 283. (d) Gromada, J.; Mortreux, A.; Carpentier, J.-F. *Coord. Chem. Rev.* **2004**, *248*, 397. (e) Corradini, P.; Guerra, G.; Cavallo, L. *Acc. Chem. Res.* **2004**, *37*, 231. (f) Kol, M.; Tshuva, E. Y.; Goldschmidt, Z. *ACS Symp. Ser.* **2003**, *857*, 62. (g) Kol, M.; Segal, S.; Groysman, S. In *Stereoselective Polymerization with Single-Site Catalysts*; CRC Press LLC: Boca Raton, FL, 2008; pp 345−361. (h) Gueta-Neyroud, T.; Tumanskii, B.; Kapon, M.; Eisen, M. S. *Macromolecules* **2007**, *40*, 5261. (i) Okuda, J. *Stud. Surf. Sci. Catal.* **2007**, *172*, 11. (j) Matsugi, T.; Fujita, F. *Chem. Soc. Rev.* **2008**, *37*, 1264. (k) Coates, G. W.; Hustad, P. D.; Reinartz, S. *Angew. Chem., Int. Ed.* **2002**, *41*, 2236. (l) Domski, G. J.; Rose, J. M.; Coates, G. W.; Bolig, A. D.; Brookhart, M. *Prog. Polym. Sci.* **2007**, *32*, 30. (m) Chan, M. C. W.; Kui, S. C. F.; Cole, J. M.; McIntyre, G. J.; Matsui, S.; Zhu, N.; Tam, K. H. *Chem.−Eur. J.* **2006**, *12*, 2607.

10.1021/om8009409 CCC: $40.75
Publication on Web 01/02/2009

Chart 1. {ON^{R1,R2}}H and {ON^{Et}NO}H$_2$ Pro-ligands Used in This Study

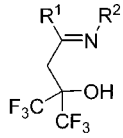

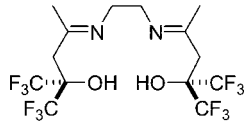

$R^1 = CH_3$, $R^2 = C_6H_5$	{ON^{Me,Ph}}H
$R^1 = CH_3$, $R^2 = C_6F_5$	{ON^{Me,ArF}}H
$R^1 = C_6H_5$, $R^2 = C_6H_5$	{ON^{Ph,Ph}}H
$R^1 = C_6H_5$, $R^2 = CH_2C_6H_5$	{ON^{Ph,Bn}}H

{ON^{Et}NO}H$_2$

structurally reminiscent of aryloxide-bearing salen[7] and phenoxyimine[2j,8,9] ligands. Those {ON^{R1,R2}}$^-$ and {ON^{Et}NO}$^{2-}$ ligands (Chart 1) enabled the preparation of discrete complexes of trivalent metals such as Y(III), La(III),[10] and Al(III),[11] conferring a high electrophilicity to the metal centers, that proved to be useful in the controlled ring-opening polymerization of cyclic esters.

We report in this article the preparation, structural characterization, and reactivity of tetravalent group 4 metal complexes supported by {ON^{R1,R2}}$^-$ and {ON^{Et}NO}$^{2-}$ ligands. Preliminary studies on the catalytic performances of such discrete complexes in ethylene polymerization are also reported, and discussed in connection with some decomposition pathways.

Results and Discussion

Several routes to Ti, Zr, and Hf complexes based on a variety of bidentate monoanionic {ON^{R1,R2}}$^-$ ligands, as well as on the tetradentate dianionic {ON^{Et}NO}$^{2-}$ ligand, have been explored: (a) σ-bond metathesis (alcoholysis) reactions between the alcohol/diol pro-ligands {ON^{R1,R2}}H and {ON^{Et}NO}H$_2$ and an appropriate homo- or heteroleptic metal precursor, enabling either alkane or alcohol elimination; (b) salt elimination reactions between {ON^{R1,R2}}M alkali metal salts, either preliminary prepared or *in situ*-generated, and a MCl$_4$(THF)$_n$ precursor. These results are discussed hereafter and summarized in Schemes 1−7. The prepared neutral complexes are all air- and moisture-sensitive[12] and were characterized in the solid state by elemental analysis and X-ray diffraction studies for some of them, and in solution by variable-temperature ^{1}H, ^{13}C, and ^{19}F NMR spectroscopy.

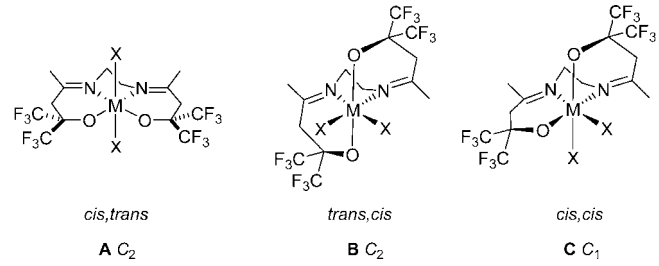

Figure 1. Possible isomers for octahedral {ON^{Et}NO}MX$_2$ complexes. The *cis/trans* descriptors refer to the arrangement of alkoxide and X ligands, respectively. Note that the imino ligands must be *cis*. Only one of the possible enantiomers (Λ, Δ, depending on the absolute configuration of the metal)[14] is depicted.

Synthesis and Structures of Neutral {ON^{Et}NO}MX$_2$ Complexes. First investigations were carried out using the tetradentate ligand {ON^{Et}NO}$^{2-}$. Assuming an ideal octahedral arrangement and flexibility of the {ON^{Et}NO}$^{2-}$ ligand framework, three {ON^{Et}NO}MX$_2$ isomeric structures are possible (**A**−**C**, Figure 1), which differ in the arrangement (*cis* vs *trans*) of the pairs of alkoxide and X ligands.[13]

The 1:1 reaction between diol {ON^{Et}NO}H$_2$ and Ti(O*i*Pr)$_2$Cl$_2$, *in situ*-generated from TiCl$_4$ and Ti(O*i*Pr)$_4$,[15] proceeded selectively at room temperature to yield {ON^{Et}NO}TiCl$_2$ (**1**), as is

(3) For selected examples of early transition metal complexes bearing fluorous alkoxide ligands: (a) Bradley, D. C.; Chudszynska, H.; Hursthouse, M. B.; Motevalli, M. *Polyhedron* **1994**, *12*, 1907. (b) Bradley, D. C.; Chudszynska, H.; Hursthouse, M. B.; Motevalli, M. *Polyhedron* **1994**, *13*, 7. (c) Samuels, J. A.; Lobkovsky, E. B.; Streib, W. E.; Folting, K.; Huffman, J. C.; Zwanziger, J. W.; Caulton, K. G. *J. Am. Chem. Soc.* **1993**, *115*, 5093. (d) Tsukuhara, T.; Swenson, D. C.; Jordan, R. F. *Organometallics* **1997**, *16*, 3303. (e) Fujimura, O.; Grubbs, R. J. *J. Am. Chem. Soc.* **1996**, *118*, 2499. (f) Fujimura, O.; De la Mata, F. J.; Grubbs, R. H. *Organometallics* **1996**, *15*, 1865.

(4) (a) Lavanant, L.; Chou, T.-Y.; Chi, Y.; Lehmann, C. W.; Toupet, L.; Carpentier, J.-F. *Organometallics* **2004**, *23*, 5450. (b) Amgoune, A.; Lavanant, L.; Thomas, C. M.; Chi, Y.; Welter, R.; Dagorne, S.; Carpentier, J.-F. *Organometallics* **2005**, *24*, 6279. (c) Kirillov, E.; Lavanant, L.; Thomas, C. M.; Roisnel, T.; Chi, Y.; Carpentier, J.-F. *Chem.−Eur. J.* **2007**, *13*, 923.

(5) Marquet, N.; Grunova, E.; Kirillov, E.; Bouyahyi, M.; Thomas, C. M.; Carpentier, J.-F. *Tetrahedron* **2008**, *64*, 75.

(6) Fluorous alkoxy-imino ligands were first prepared in the coordination sphere of metals ions, i.e., Cu^{2+}, Ni^{2+}, Co^{2+}, Ce^{3+}, Ce^{4+} by the template condensation of primary (di)amines with the fluorous β-ketol MeC(=O)CH$_2$C(CF$_3$)$_2$OH; see: (a) Martin, J. W. L.; Willis, C. J. *Can. J. Chem.* **1977**, *55*, 2459. (b) Konefal, E.; Loeb, S. J.; Stephan, D. W.; Willis, C. J. *Inorg. Chem.* **1984**, *23*, 538, and references therein.

(7) (a) Jacobsen, E. N. *Catalytic Asymmetric Synthesis*; OjimaI., Ed.; VCH: Weinheim, 1993; p 159. (b) Jacobsen, E. N. *Comprehensive Organometallic Chemistry II*; Wilkinson, G.; Stone, F. G. A.; Abel, E. W.; Hegedus, L. S., Eds.; Pergamon Press: New York, 1995; Vol. 12,Chapter 11.1. (c) Larrow, J. F.; Jacobsen, E. N. *Top. Organomet. Chem.* **2004**, *6*, 123. (d) Cozzi, P. G. *Chem. Soc. Rev.* **2004**, *33*, 410. (e) Katsuki, T. *Chem. Soc. Rev.* **2004**, *33*, 437. (f) Atwood, D. A.; Harvey, M. J. *Chem. Rev.* **2001**, *101*, 37.

(8) (a) Makio, H.; Fujita, T. *Macromol. Rapid Commun.* **2007**, *28*, 698. (b) Terao, H.; Ishii, S.; Saito, J.; Matsuura, S.; Mitani, M.; Nagai, N.; Tanaka, H.; Fujita, T. *Macromolecules* **2006**, *39*, 8584. (c) Nakayama, Y.; Saito, J.; Bando, H.; Fujita, T. *Chem.−Eur. J.* **2006**, *12*, 7546. (d) Saito, J.; Suzuki, Y.; Makio, H.; Tanaka, H.; Onda, M.; Fujita, T. *Macromolecules* **2006**, *39*, 4023. (e) Mitani, M.; Nakano, T.; Fujita, T. *Chem.−Eur. J.* **2003**, *9*, 2396. (f) Mitani, M.; Furuyama, R.; Mohri, J.; Saito, J.; Ishii, S.; Terao, H.; Nakano, T.; Tanaka, H.; Fujita, T. *J. Am. Chem. Soc.* **2003**, *125*, 4293. (g) Makio, H.; Kashiwa, N.; Fujita, T. *Adv. Synth. Catal.* **2002**, *344*, 477. (h) Mitani, M.; Furuyama, R.; Mohri, J.; Saito, J.; Ishii, S.; Terao, H.; Kashiwa, N.; Fujita, T. *J. Am. Chem. Soc.* **2002**, *124*, 7888. (i) Mitani, M.; Mohri, J.; Yoshida, Y.; Saito, J.; Ishii, S.; Tsuru, K.; Matsui, S.; Furuyama, R.; Nakano, T.; Tanaka, H.; Kojoh, S.; Matsugi, T.; Kashiwa, N.; Fujita, T. *J. Am. Chem. Soc.* **2002**, *124*, 3327. (j) Saito, J.; Mitani, M.; Mohri, J.; Yoshida, Y.; Matsui, S.; Ishii, S.; Kojoh, S.; Kashiwa, N.; Fujita, T. *Angew. Chem., Int. Ed.* **2001**, *40*, 2918. (k) Matsui, S.; Mitani, M.; Saito, J.; Tohi, Y.; Makio, H.; Matsukawa, N.; Takagi, Y.; Tsuru, K.; Nitabaru, M.; Nakano, T.; Tanaka, H.; Kashiwa, N.; Fujita, T. *J. Am. Chem. Soc.* **2001**, *123*, 6847.

(9) (a) Mason, A. F.; Coates, G. W. *J. Am. Chem. Soc.* **2004**, *126*, 10798. (b) DeRosa, C.; Circelli, T.; Auriemma, F.; Mathers, R. T.; Coates, G. W. *Macromolecules* **2004**, *37*, 9034. (c) Mason, A. F.; Coates, G. W. *J. Am. Chem. Soc.* **2004**, *126*, 16326. (d) Reinartz, S.; Mason, A. F.; Lobkovsky, E. B.; Coates, G. W. *Organometallics* **2003**, *22*, 2542. (e) Hustad, P. D.; Tian, J.; Coates, G. W. *J. Am. Chem. Soc.* **2002**, *124*, 3614. (f) Tian, J.; Coates, G. W. *Angew. Chem., Int. Ed.* **2000**, *39*, 3626.

(10) Grunova, E.; Kirillov, E.; Roisnel, T.; Carpentier, J.-F. *Organometallics* **2008**, *27*, 5691.

(11) Bouyahyi, M.; Grunova, E.; Marquet, N.; Kirillov, E.; Thomas, C. M.; Roisnel, T.; Carpentier, J.-F. *Organometallics* **2008**, *22*, 5815−5825.

(12) Benzyl complexes of zirconium and hafnium proved also to be sensitive when exposed to light, as solutions in hydrocarbons.

(13) Sanz, M.; Cuenca, T.; Cuomo, C.; Grassi, A. *J. Organomet. Chem.* **2006**, *691*, 3816, and references therein.

(14) Purcell, K. F.; Kotz, J. C. In *Inorganic Chemistry*; Saunders Co.: Philadelphia, 1977; pp 368−648.

(15) Gothelf, K. V.; Jorgensen, K. A. *J. Org. Chem.* **1994**, *59*, 5687.

Scheme 1

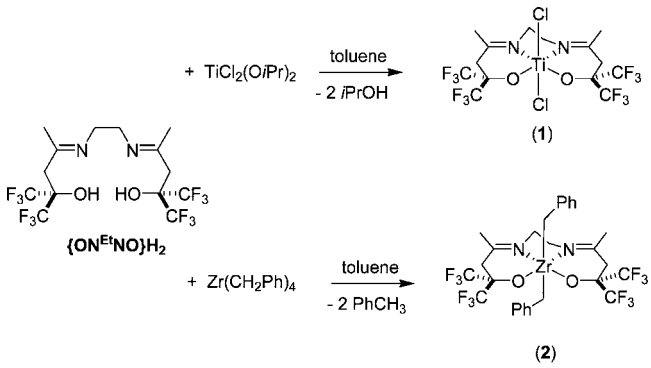

common of simple exchange reactions between titanium alkoxide complexes and alcohols.[1] Similarly, the dibenzyl complex $\{ON^{Et}NO\}Zr(CH_2Ph)_2$ (**2**) was prepared by alcoholysis of $Zr(CH_2Ph)_4$ (Scheme 1). Both complexes are sparingly soluble in aliphatic hydrocarbons (pentane, hexanes) but readily soluble in aromatic hydrocarbons (benzene, toluene) and chlorinated solvents (CH_2Cl_2), in which they are stable for at least weeks at room temperature.

Crystals of **1** suitable for X-ray diffraction were obtained from a toluene solution. The solid-state structure of **1** (Figure 2) features a monomeric molecule with a six-coordinated metal center and equatorial coordination of the $\{ON^{Et}NO\}^{2-}$ ligand, in a Salen-like fashion, that is a type **A** structure (Figure 1). We have observed a similar planar coordination mode when exploring the aluminum chemistry of this ligand, although the square-pyramidal (sqp) geometry structures of these Al complexes are more distorted toward a trigonal-bipyramidal (tbp) geometry.[7f,11] However, the most worthy and meaningful structural comparison for these new diimino-diolate complexes is undoubtedly with group 4 metal salen (i.e., diiminobisphenolate) complexes, since both incorporate similar ligand frameworks. In fact, the metrical data in **1**, i.e., bond distances Ti−O (1.819(3)−1.822(3) Å), Ti−N (2.173(4)−2.182(4) Å), and Ti−Cl (2.3368(14)−2.3372(15) Å) and the corresponding bond angles O−Ti−O (108.61(14)°), N−Ti−N (76.63(13)°), and Cl−Ti−Cl (165.00(6)°) (Figure 1), compare very well with those observed in related ethylene- and 1,2-cyclohexylene-bridged-Salen dichlorotitanium complexes [Ti−O (1.816−1.844 Å), Ti−N (2.121−2.171 Å), Ti−Cl (2.326−2.370 Å), O−Ti−O (110.05−113.27°), N−Ti−N (75.29−78.91°), Cl−Ti−Cl (168.21−171.42°)].[16] The Ti, O, O, N, N atoms are almost perfectly coplanar (maximum deviation from mean plane: 0.022 Å). Also, the six-membered metallacycles involving the imino-alkoxide ligand in **1** appear quite planar (deviation from the mean plane Ti−N−C−C−C−O: Ti(1), −0.076; O(11), +0.059, C(11), +0.204; C(14), −0.314; C(15), +0.072; N(17), +0.154 Å). These data indicate that substitution of a phenoxide group for a bis(trifluoromethyl)alkoxide group did not affect significantly the coordination mode, although there is no more conjugation with the imino moiety in complex **1**. On the other hand, the solid-state structure of **1** differs dramatically from that observed for the related fluorous dialkoxide-*diamino* complex $\{CH_2NMeCH_2C(CF_3)_2O\}_2TiCl_2$ and $\{CH_2NMeCH_2C(CF_3)_2O\}_2Zr(CH_2Ph)_2$.[4a] In fact, the latter complexes adopt also a distorted octahedral geometry but in which the oxygen atoms of the dialkoxide ligand are *trans* and the X ligands (X = Cl, CH_2Ph, respectively) are *cis*; that is a type **B** structure (Figure 1). This observation suggests that substitution of an amino for an imino group is more crucial in terms of ligand framework flexibility than the aforementioned modification (substitution of a phenoxide group for a bis(trifluoromethyl)alkoxide group) and does not induce significant constraint within the six-membered N−M−O metallacycles.

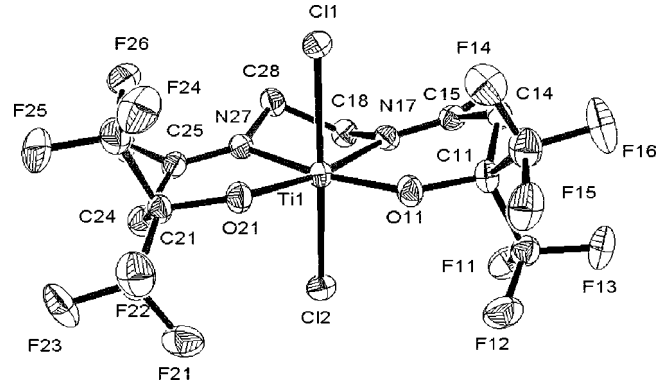

Figure 2. ORTEP view of $\{ON^{Et}NO\}TiCl_2$ (**1**) (ellipsoids drawn at the 50% probability level; all hydrogen atoms have been omitted for clarity). Selected bond lengths (Å) and angles (deg): Ti(1)−O(21), 1.819(3); Ti(1)−O(11), 1.822(3); Ti(1)−N(17), 2.173(4); Ti(1)−N(27), 2.182(4); Ti(1)−Cl(1), 2.3368(14); Ti(1)−Cl(2), 2.3372(15); O(21)−Ti(1)−O(11), 108.61(14); O(21)−Ti(1)−N(17), 163.85(14); O(11)−Ti(1)−N(17), 87.36(14); O(21)−Ti(1)−N(27), 87.38(13); O(11)−Ti(1)−N(27), 163.99(13); N(17)−Ti(1)−N(27), 76.63(13); O(21)−Ti(1)−Cl(1), 93.35(11); O(11)−Ti(1)−Cl(1), 93.36(11); N(17)−Ti(1)−Cl(1), 83.07(10); N(27)−Ti(1)−Cl(1), 84.84(11); O(21)−Ti(1)−Cl(2), 95.41(11); O(11)−Ti(1)−Cl(2), 95.35(11); N(17)−Ti(1)−Cl(2), 85.15(10); N(27)−Ti(1)−Cl(2), 83.42(11); Cl(1)−Ti(1)−Cl(2), 165.00(6).

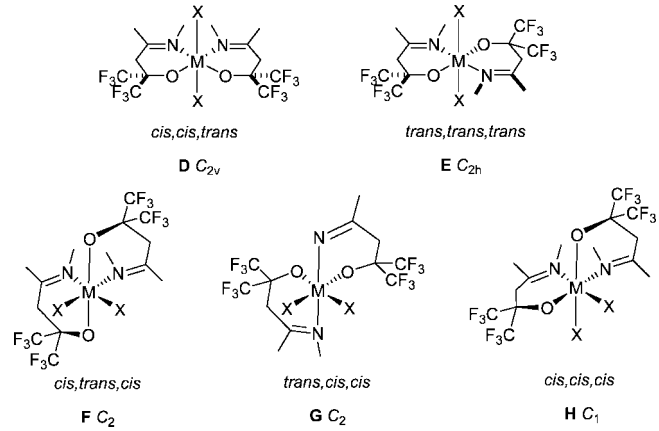

Figure 3. Possible isomers for octahedral $\{ON^{R1,R2}\}MX_2$ complexes. The *cis/trans* descriptors refer to the arrangement of imino, alkoxide, and X ligands, respectively. Enantiomers of C_2- and C_1-symmetric isomers are not depicted. R^1 and R^2 substituents are not shown for the sake of clarity.

In agreement with the structure observed in the solid state, the ^1H, ^{13}C, and ^{19}F NMR data for **1** in CD_2Cl_2 at room temperature contain a single set of resonances, consistent with an average C_{2v}-symmetric type **A** structure retained in solution. In particular, the ^1H NMR spectrum contains three singlet resonances for the CH_3, $CH_2C{=}N$, and NCH_2 groups, respectively, while only one singlet resonance is observed for the $OC(CF_3)_2$ moieties in the $^{19}F\{^1H\}$ NMR spectrum.[17] No fluxional dynamic process associated with possible isomerization of the ligand backbone in **1** was observed by VT ^1H NMR in the temperature range −60 to 60 °C.

Single crystals of **2** suitable for X-ray diffraction studies could not be obtained, and this complex was characterized in solution by NMR spectroscopy. The ^1H, ^{13}C, and ^{19}F NMR data for **2** in

Scheme 2

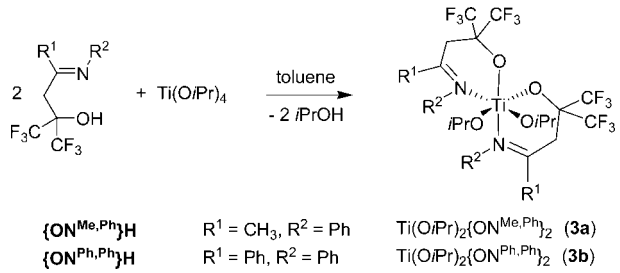

CD_2Cl_2 at room temperature are very similar to those observed for **1** and include a sharp singlet resonance in the $^{19}F\{^1H\}$ NMR spectrum, as well as three singlets in the ^1H spectrum for the ligand hydrogens. In addition, the benzyl groups appear as a single singlet resonance in both the ^1H and ^{13}C NMR spectra. These data are consistent with an average C_{2v}-symmetric type **A** structure, with equatorial coordination of the $\{ON^{Et}NO\}^{2-}$ ligand, as observed for **1**.[17]

Synthesis, Structures, and Reactivity of Neutral $\{ON^{R,R}\}MX_2$ Complexes. We turned our attention next to the coordination of monoanionic bidentate ligands $\{ON^{R1,R2}\}^-$. In this case, up to five isomeric structures (without considering enantiomers) can be envisaged (Figure 3).[13]

Isopropoxide and Chloride Complexes of Titanium. Due to easiness of alcohol elimination processes[1] and their efficiency demonstrated in the above-mentioned formation of $\{ON^{Et}NO\}$-$TiCl_2$ (**1**), this route was also explored to prepare related diisopropoxide titanium complexes based on monoanionic bidentate ligands $\{ON^{R1,R2}\}^-$. In fact, alcoholysis of $Ti(OiPr)_4$ with 2 equiv of fluorinated alcohol-imines $\{ON^{R1,R2}\}H$ (R^1 = CH_3, Ph; R^2 = Ph) proceeds fast and selectively, at room temperature in toluene or benzene, to afford the corresponding $Ti(OiPr)_2\{ON^{R1,R2}\}_2$ complexes **3a** and **3b**, with concomitant release of 2 equiv of 2-propanol (Scheme 2). Complexes **3a** and **3b** were isolated in 63% and 64% yields, respectively, and are both colorless compounds, readily soluble in most common organic solvents, and thermally stable both in solution and in the solid state in the absence of air.

Crystals of **3a** suitable for X-ray diffraction were grown from a toluene/hexane solution. The molecular structure of **3a** (Figure 4) features a monomeric complex in a distorted octahedral geometry, with a *cis,cis,cis* arrangement of the nitrogen ligand atoms, oxygen ligand atoms, and isopropoxide groups, which is a type **H** structure (Figure 3). The Ti−O (1.894−1.974(1) Å) and Ti−N (2.279−2.374(2) Å) bonds involving the ligand atoms in **3a** are significantly longer than those observed in **1** (*vide supra*; Figure 2) and in related titanium-Salen complexes.[16,18]

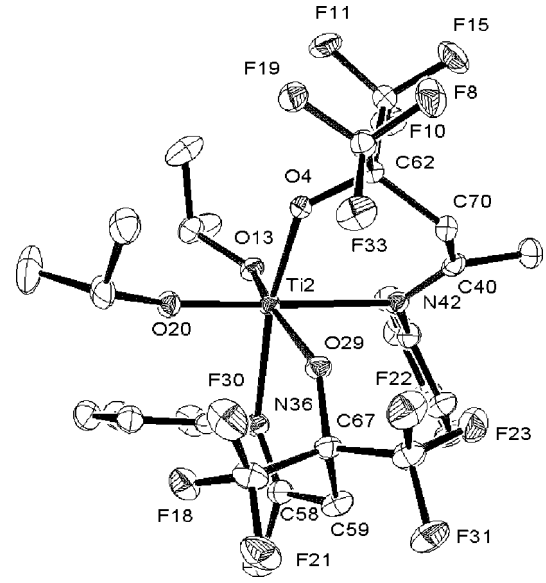

Figure 4. ORTEP view of $Ti(OiPr)_2\{ON^{Me,Ph}\}_2$ (**3a**) (ellipsoids drawn at the 50% probability level; all hydrogen atoms have been omitted for the sake of clarity; only one (#2) of the two independent molecules found in the unit cell is depicted). Selected bond lengths (Å) and angles (deg) [data in square brackets refer to the second independent molecule (#1)]: Ti(2)−O(20), 1.7791(14) [1.8066(14)]; Ti(2)−O(13), 1.8337(13) [1.8128(13)]; Ti(2)−O(4), 1.8947(13) [1.9109(13)]; Ti(2)−O(29), 1.9537(13) [1.9741(13)]; Ti(2)−N(36), 2.2817(17) [2.2794(16)]; Ti(2)−N(42), 2.3428(17) [2.3744(17)]; O(20)−Ti(2)−O(13), 96.88(6) [94.40(6)]; O(20)−Ti(2)−O(4), 96.77(6) [94.49(6)]; O(13)−Ti(2)−O(4), 98.37(6) [99.58(6)]; O(20)−Ti(2)−O(29), 98.92(6) [95.85(6)]; O(13)−Ti(2)−O(29), 160.54(6) [163.49(6)]; O(4)−Ti(2)−O(29), 90.99(6) [92.49(5)]; O(20)−Ti(2)−N(36), 91.75(6) [97.71(6)]; O(13)−Ti(2)−N(36), 86.91(6) [84.22(6)]; O(4)−Ti(2)−N(36), 169.34(6) [166.91(6)]; O(29)−Ti(2)−N(36), 81.34(6) [81.61(5)]; O(20)−Ti(2)−N(42), 177.95(6) [175.93(5)]; O(13)−Ti(2)−N(42), 81.20(6) [84.13(6)]; O(4)−Ti(2)−N(42), 82.84(6) [82.04(6)]; O(29)−Ti(2)−N(42), 83.10(6) [86.46(5)]; N(36)−Ti(2)−N(42), 88.86(6) [85.93(6)].

Also, the O−Ti−N angles (81.34(6)−82.84(6)°) in the six-membered metallacycles of **3a** are smaller than those in **1** (87.36(14)−87.38(13)°). Those differences in metrical data probably reflect, in main part, the influence of the bridging unit in between the two alkoxy-imino moieties and possibly the *trans* influence of ligands as well. On the other hand, these bond distances and bond angles in **3a** compare well with those found in diisopropoxide and other dialkoxide titanium complexes supported by phenoxy-imine ligands (Ti−O, 1.895−1.975 Å; Ti−N, 2.228−2.340 Å; O−Ti−N, 79.73−82.34°).[19] Both the

Scheme 3

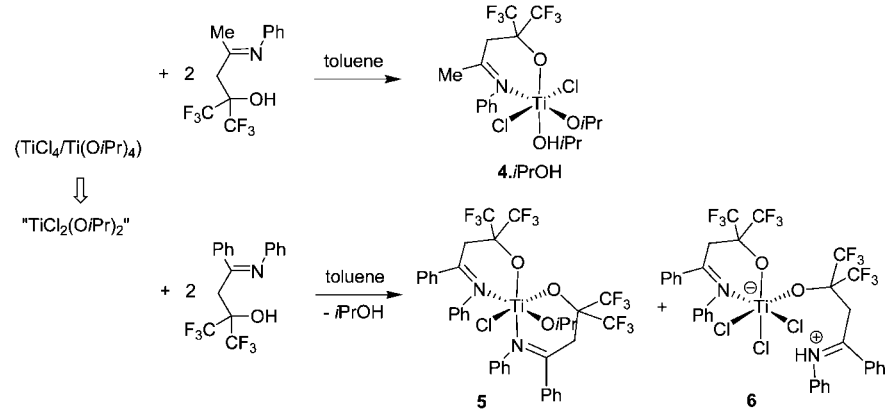

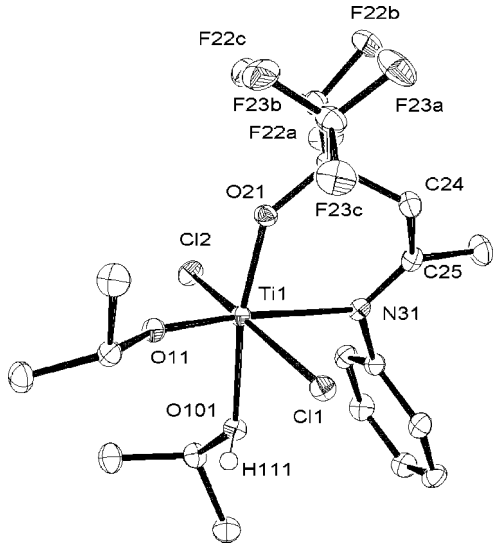

Figure 5. ORTEP view of $TiCl_2(OiPr)\{ON^{Me,Ph}\}\cdot i$PrOH (**4**·*i*PrOH) (ellipsoids drawn at the 50% probability level; all hydrogen atoms except H(111) have been omitted for the sake of clarity). Selected bond lengths (Å) and angles (deg): Ti(1)−O(11), 1.7440(11); Ti(1)−O(21), 1.8411(11); Ti(1)−O(101), 2.1338(12); Ti(1)−N(31), 2.2967(13); Ti(1)−Cl(2), 2.3206(5); Ti(1)−Cl(1), 2.4179(5); O(11)−Ti(1)−O(21), 96.81(5); O(11)−Ti(1)−O(101), 93.06(5); O(21)−Ti(1)−O(101), 169.32(5); O(11)−Ti(1)−N(31), 170.38(5); O(21)−Ti(1)−N(31), 83.90(5); O(101)−Ti(1)−N(31), 85.68(5); O(11)−Ti(1)−Cl(2), 101.71(4); O(21)−Ti(1)−Cl(2), 94.38(4); O(101)−Ti(1)−Cl(2), 87.54(3); N(31)−Ti(1)−Cl(2), 87.78(4); O(11)−Ti(1)−Cl(1), 90.48(4); O(21)−Ti(1)−Cl(1), 94.94(4); O(101)−Ti(1)−Cl(1), 80.90(3); N(31)−Ti(1)−Cl(1), 79.90(3); Cl(2)−Ti(1)−Cl(1), 163.654(18).

six-membered metallacycles appear rather planar, apart from the "central" CH_2 carbon that deviates significantly from the mean plane Ti−N−C−C−C−O (C(70), 0.154 Å; C(59), 0.265 Å; all other deviations in the range 0.003−0.117 Å).

The ^{1}H, ^{13}C, and ^{19}F NMR data for **3a** and **3b**, in C_6D_6 or CD_2Cl_2 at room temperature, are very similar. For both complexes, a single sharp singlet resonance in the ^{19}F{^{1}H} NMR spectrum as well as three singlets in the ^{1}H NMR spectrum for the CH_3, $CH_2C{=}N$, and NCH_2 hydrogens in the ligand are observed. No change is observed in the low-temperature (−50 °C) ^{1}H NMR spectrum of **3a** and **3b** in CD_2Cl_2. These features, which are confirmed in the ^{13}C NMR spectra, are consistent with the existence of a single C_{2v}-symmetric structure on the NMR time scale[17] (type **D**, Figure 3) and indicate that the solid-state structure observed for **3a** is not retained in solution.

Similar alcoholysis reactions were investigated using *in situ*-generated $Ti(OiPr)_2Cl_2$ instead of $Ti(OiPr)_4$ in an attempt to prepare the corresponding dichloride complexes.[20] However, in contrast with the clean formation of **1** and **3a**,**b**, those reactions proved to be not as selective as expected. The reaction of 2 equiv of $\{ON^{Me,Ph}\}H$ with $Ti(OiPr)_2Cl_2$ led to the immediate precipitation of the adduct $TiCl_2(OiPr)\{ON^{Me,Ph}\}\cdot i$PrOH (**4**·*i*PrOH), which results obviously from the alcoholysis of a single isopropoxide group (Scheme 3). Once isolated and dried under vacuum, this complex rapidly loses its coordinated 2-propanol molecule to give **4**, as confirmed by NMR spectroscopy. Change of the reaction conditions (prolonged heating, solvent) did not allow accessing the targeted $TiCl_2\{ON^{Me,Ph}\}_2$ complex. On the other hand, repeated reactions of 2 equiv of $\{ON^{Ph,Ph}\}H$ with $Ti(OiPr)_2Cl_2$ led systematically to complex mixtures of compounds (as judged by ^{1}H and ^{19}F NMR). Recrystallization of crude products afforded only small amounts of crystals, which

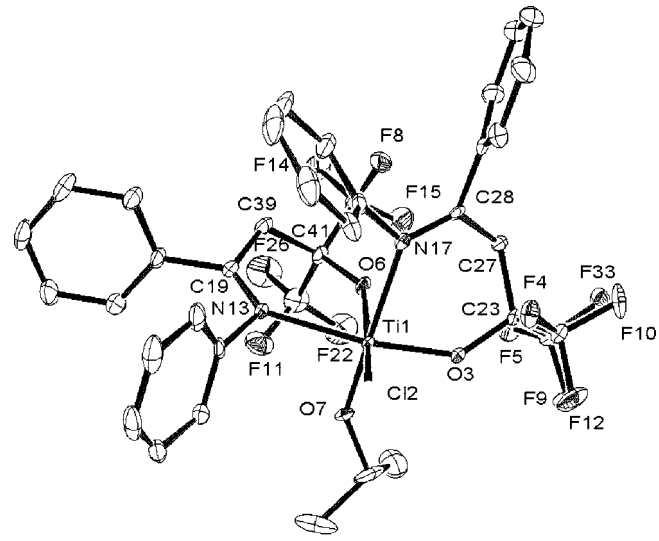

Figure 6. ORTEP view of $TiCl(OiPr)\{ON^{Ph,Ph}\}_2$ (**5**) (ellipsoids drawn at the 50% probability level; all hydrogen atoms have been omitted for the sake of clarity). Selected bond lengths (Å) and angles (deg): Ti(1)−O(7), 1.749(2); Ti(1)−O(3), 1.8519(19); Ti(1)−O(6), 1.884(2); Ti(1)−N(13), 2.260(2); Ti(1)−Cl(2), 2.3428(9); Ti(1)−N(17), 2.376(2); O(7)−Ti(1)−O(3), 96.31(9); O(7)−Ti(1)−O(6), 99.16(9); O(3)−Ti(1)−O(6), 93.49(8); O(7)−Ti(1)−N(13), 91.99(9); O(3)−Ti(1)−N(13), 171.32(9); O(6)−Ti(1)−N(13), 82.65(9); O(7)−Ti(1)−Cl(2), 95.03(8); O(3)−Ti(1)−Cl(2), 92.62(6); O(6)−Ti(1)−Cl(2), 163.82(7); N(13)−Ti(1)−Cl(2), 89.17(7); O(7)−Ti(1)−N(17), 179.61(10); O(3)−Ti(1)−N(17), 83.36(8); O(6)−Ti(1)−N(17), 80.67(8); N(13)−Ti(1)−N(17), 88.34(8); Cl(2)−Ti(1)−N(17), 85.18(6).

turned out to be mixtures of the mixed chloride-isopropoxide complex $TiCl(OiPr)\{ON^{Ph,Ph}\}_2$ (**5**)[21] and the zwitterionic complex $[TiCl_3\{ON^{Ph,Ph}\}\{ONH^{Ph,Ph}\}]$ (**6**) (Scheme 3). In the latter complex, one of the two ligand units is coordinated by a single σ-alkoxide group, while its imino function has been protonated.

Complexes **4**·*i*PrOH, **5**, and **6** were structurally characterized by X-ray diffraction studies (Figures 5 −7 Table 1). The main Ti−$\{ON^{R1,R2}\}$, Ti−O*i*Pr, and Ti−Cl bond distances and related angles in these three complexes are quite similar to those discussed above for complexes **1** and **3a**. As in the case of **3a**, complex **5** features a type **H** structure. Peculiarities in **4**·*i*PrOH

(16) (a) Tararov, V. I.; Hibbs, D. E.; Hursthouse, M. B.; Ikonnikov, N. S.; Malik, K. M. A.; North, M.; Orizu, C.; Belokon, Y. N. *Chem. Commun.* **1998**, 387. (b) Gilli, G.; Cruickshank, D. W. J.; Beddoes, R. L.; Mills, O. S. *Acta Crystallogr., B Struct. Crystallogr. Cryst. Chem.* **1972**, *28*, 1889. (c) Repo, T.; Klinga, M.; Leskela, M.; Pietikainen, P.; Brunow, G. *Acta Crystallogr. C: Cryst. Struct. Commun.* **1996**, *52*, 2742. (d) Kim, I.; Ha, Y. S.; Zhang, D. F.; Ha, C.-S.; Lee, U. *Macromol. Rapid Commun.* **2004**, *25*, 1319. (e) Choudhary, N. F.; Hitchcock, P. B.; Leigh, G. J. *Inorg. Chim. Acta* **2000**, *306*, 24. (f) Kelly, D. G.; Toner, A. J.; Walker, N. M.; Coles, S. J.; Hursthouse, M. B. *Polyhedron* **1996**, *15*, 4307.

(17) In a C_2-symmetric environment such as in structure **B** (Figure 1), **D**, or **E** (Figure 3), two doublets are expected for the diastereotopic hydrogens of the C*HH* ligand unit adjacent, as well as for the diastereotopic hydrogens of C*HH*Ph groups in dibenzyl complexes **7** and **8**. Also, the ^{19}F NMR spectrum would feature two quartets for the nonequivalent $C(CF_3)(CF_3)$ groups; see refs 4a,b.

(18) Gregson, C. K. A.; Blackmore, I. J.; Gibson, V. C.; Long, N. J.; Marshall, E. L.; White, A. J. P. *Dalton Trans.* **2006**, 3134.

(19) (a) Fleischer, R.; Wunderlich, H.; Braun, M. *Eur. J. Org. Chem.* **1998**, 1063. (b) Braun, M.; Hahn, A.; Engelmann, M.; Fleischer, R.; Frank, W.; Kryschi, C.; Haremza, S.; Kurschner, K.; Parker, R. *Chem.−Eur. J.* **2005**, *11*, 3405. (c) Flores-Lopez, L. Z.; Parra-Hake, M.; Somanathan, R.; Walsh, P. J. *Organometallics* **2000**, *19*, 2153. (d) Davidson, M. G.; Johnson, A. L.; Jones, M. D.; Lunn, M. D.; Mahon, M. F. *Eur. J. Inorg. Chem.* **2006**, 4449. (e) Johnson, A. L.; Davidson, M. G.; Lunn, M. D.; Mahon, M. F. *Eur. J. Inorg. Chem.* **2006**, 3088.

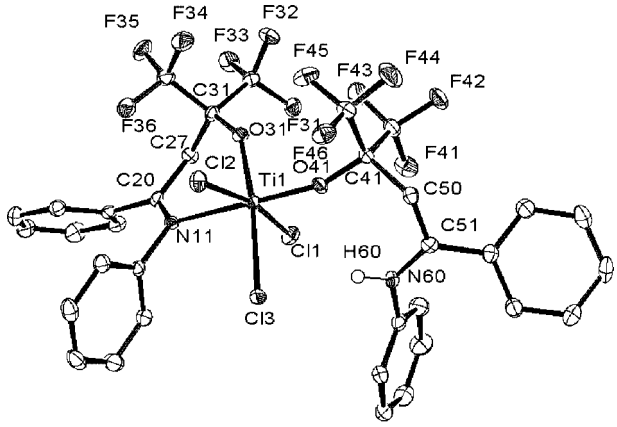

Figure 7. ORTEP view of $[TiCl_3\{ON^{Ph,Ph}\}\{ONH^{Ph,Ph}\}]$ (**6**) (ellipsoids drawn at the 50% probability level; all hydrogen atoms have been omitted for the sake of clarity, except the one on the protonated imino function). Selected bond lengths (Å) and angles (deg): Ti(1)−O(41), 1.8298(16); Ti(1)−O(31), 1.8358(16); Ti(1)−N(11), 2.3020(19); Ti(1)−Cl(2), 2.3394(7); Ti(1)−Cl(1), 2.3608(8); Ti(1)−Cl(3), 2.3873(7); O(41)−Ti(1)−O(31), 96.80(7); O(41)−Ti(1)−N(11), 178.84(7); O(31)−Ti(1)−N(11), 82.69(7); O(41)−Ti(1)−Cl(2), 94.80(5); O(31)−Ti(1)−Cl(2), 92.78(6); N(11)−Ti(1)−Cl(2), 86.27(5); O(41)−Ti(1)−Cl(1), O(31)−Ti(1)−Cl(1), 92.64(6); N(11)−Ti(1)−Cl(1), 83.98(5); Cl(2)−Ti(1)−Cl(1), 168.15(3); O(41)−Ti(1)−Cl(3), 91.71(5); O(31)−Ti(1)−Cl(3), 171.33(6); N(11)−Ti(1)−Cl(3), 88.77(5); Cl(2)−Ti(1)−Cl(3), 88.13(3); Cl(1)−Ti(1)−Cl(3), 84.95(3).

involve an expectedly longer Ti−OH*i*Pr bond distance (2.134(1) Å) (as compared to Ti−O*i*Pr, 1.744(1) Å) and a more acute Ti−O−C bond angle (131.68(9)° vs 151.31(11)°, respectively). The presence of the 2-propanol molecule also likely accounts for the reduced *trans* Ti−O(ligand) bond distance of 1.841(1) Å, as compared to that of 1.954(1) Å for the Ti−O(ligand) *trans* to an isopropoxide group in complex **3a**. In zwitterionic complex **6**, there is a short Cl(3)···H(60)−N(60) contact of 2.439 Å.

Dibenzyl Complexes of Zirconium and Hafnium. Dibenzyl complexes of zirconium and hafnium based on monoanionic bidentate ligands $\{ON^{R1,R2}\}^-$ were prepared by alcoholysis of $Zr(CH_2Ph)_4$ and $Hf(CH_2Ph)_4$ with 2 equiv of fluorous alcohol-imines $\{ON^{R1,R2}\}H$. These reactions proceed very fast and selectively, in toluene at low temperature (<−30 °C), to afford the corresponding $M(CH_2Ph)_2\{ON^{R1,R2}\}_2$ complexes (M = Zr, **7**; M = Hf, **8**), with concomitant release of 2 equiv of toluene (Scheme 4). However, these compounds subsequently decompose at higher temperature ($-30 < T$ (°C) < 20), within minutes to days depending on the nature of the ligand and the metal, by abstraction of a hydrogen from the methylene ligand backbone by a benzyl group.[12,20,22] This process is rather selective [main or only decomposition process observed; see Experimental Section] and eventually results in the release of a toluene molecule and the formation of $M(CH_2Ph)\{ON^{R1,R2}\}\{ON^{-R1,R2}\}$ complexes (M = Zr, **9**; M = Hf, **10**) in which a ligand unit ($\{ON^{-R1,R2}\}$) now acts as an α,β-unsaturated amido-alkoxy dianionic moiety (Scheme 5). This process differs fundamentally from the one observed in related Schiff base zirconium alkyls, which decompose via migration (1,2-migratory insertion or radical) of an alkyl group to imine.[23] In the present case, abstraction of a hydrogen by a nucleophilic benzyl group can be accounted for by the high acidity of the methylene group,[24] due to its substitution by electron-withdrawing α-imino and β-CF_3 groups. We cannot, however, rule out other pathways (e.g., radical)[12] at this stage. More detailed investigations, including

Scheme 4

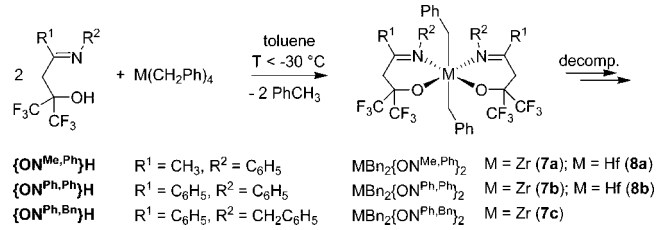

Scheme 5

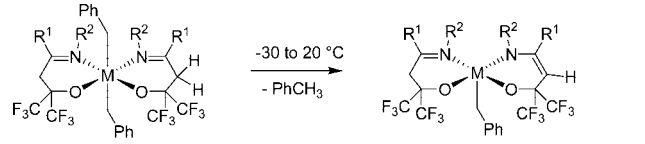

computations, are underway to further explore the origin and mechanism of this decomposition and, on the other hand, account for the thermal stability of dibenzyl complex **2** (*vide supra*).[25,26]

This facile decomposition process hampered the isolation of large amounts of analytically pure dibenzyl complexes **7** and **8**. Nonetheless, suitable crystals for X-ray diffraction of zirconium complexes **7a** and **7b** and of hafnium complex **8a** could be collected from syntheses performed at low temperature. The solid-state structures of **7a**, **7b**, and **8a** are shown in Figures 8−10. The three compounds adopt a distorted octahedral geometry with the two $\{ON^{R1,R2}\}^-$ ligand units located in the equatorial plane in a *cis*-N,N/*cis*-O,O fashion

(20) Repeated attempts under various conditions to obtain $TiCl_2\{ON^{R1,R2}\}_2$ complexes by regular salt metathesis of $TiCl_4$ (or $TiCl_4(THF)_2$) with the Li^+ (*in situ* generated), Na^+, or K^+ (isolated; see Experimental Section) salts of $\{ON^{Me,Ph}\}^-$ and $\{ON^{Ph,Ph}\}^-$ led to intractable mixtures of compounds that could not be separated nor unambiguously identified. Only in one case could small amounts of crystals be isolated, which proved by X-ray diffraction to be $TiCl_2\{ON^{Ph,Ph}\}\{OO^{Ph}\}$], where $\{OO^{Ph}\}^-$ is the aldolate ligand $[(CF_3)_2C(O)CH_2C(=O)Ph]^-$, i.e., the decomposition product of the initial ligand. Similarly, all attempts to prepare dibenzyl complexes of titanium by alcoholysis of $Ti(CH_2Ph)_4$ with 2 equiv of fluorous alcohol-imines $\{ON^{R1,R2}\}H$ led to intractable mixtures of compounds. We assume that the latter difficulties reflect the versatile redox chemistry of Ti, combined with the identified decomposition pathways of dibenzyl-metal (Zr, Hf) complexes of these new ligands. It is noteworthy that, to our knowledge, there is no dibenzyl-titanium complex of "regular" phenoxyimine ligands reported thus far; see refs 8 and 9.

(21) We observed that the reaction of 2 equiv of the aldol $(CF_3)_2C(OH)CH_2C(=O)CH_3$ ($\{OO^{Me}\}H$) (ref 5) with $Ti(OiPr)_2Cl_2$ also leads to the mixed chloride-isopropoxide complex $Ti(OiPr)Cl\{OO^{Me}\}_2$, as the main isolable product (see Experimental Section).

(22) For selected examples of decomposition pathways of early transition metal complexes involving hydrogen abstraction, see: (a) Bernskoetter, W. H.; Pool, J. A.; Lobkovsky, E.; Chirik, P. J. *Organometallics* **2006**, *25*, 1092, and references therein. (b) Schock, L. E.; Brock, C. P.; Marks, T. J. *Organometallics* **1987**, *6*, 232, and references therein. (c) Knight, L. K.; Piers, W. E.; Fleurat-Lessard, P.; Parvez, M.; McDonald, R. *Organometallics* **2004**, *23*, 2087. (d) Pattiasina, J. W.; Hissink, C. E.; de Boer, J. L.; Meetsma, A.; Teuben, J. H. *J. Am. Chem. Soc.* **1985**, *107*, 1158. (e) Skvortsov, G. G.; Fukin, G. K.; Trifonov, A. A.; Noor, A.; Doring, C.; Kempe, R. *Organometallics* **2007**, *26*, 5770.

(23) (a) Knight, P. D.; Clarkson, G.; Hammond, M. L.; Kimberley, B. S.; Scott, P. *J. Organomet. Chem.* **2005**, *690*, 5125. (b) Knight, P. D.; O'Shaughnessy, P. N.; Munslow, I. J.; Kimberley, B. S. *J. Organomet. Chem.* **2003**, *683*, 103. (c) Woodman, P. R.; Alcock, N. W.; Munslow, I. J.; Sanders, C. J.; Scott, P. *Dalton Trans.* **2000**, 3340.

(24) Reaction of $\{ON^{Me,Ph}\}H$ with 2 equiv of KH readily leads to the formation of the $\{ON^{-Me,Ph}\}K_2$, via proton abstraction from the O*H* and CH*H* groups; see Experimental Section.

Table 1. Summary of Crystal and Refinement Data for Complexes 1, 3a, 4, 5, 6, 7a, 7b, 7d, 8a, and 11

	1	**3a**	**4·*i*PrOH**	**5**	**6**
empirical formula	$C_{14}H_{14}C_{12}F_{12}N_2O_2Ti$	$C_{30}H_{34}F_{12}N_2O_4Ti$	$C_{18}H_{25}C_{12}F_6NO_3Ti$	$C_{37}H_{31}C_{11}F_{12}N_2O_3Ti$	$C_{34}H_{25}C_{13}F_{12}N_2O_2Ti.C_7H_8$
fw	589.07	762.49	536.19	862.99	967.94
cryst syst	orthorhombic	monoclinic	triclinic	monoclinic	monoclinic
space group	$P2_12_12_1$	$P2_1/a$	$P\bar{1}$	$P2_1/n$	$P2_1/c$
a, Å	11.5983(6)	19.910(4)	10.2267(9)	9.1162(9)	11.44850(10)
b, Å	13.5379(10)	16.379(4)	11.4449(11)	12.2176(12)	14.96840(10)
c, Å	13.592(9)	20.634(4)	14.0137(12)	33.617(3)	24.8484(2)
α, deg	90	90	112.483(4)	90	90
β, deg	90	95.938(10)	106.534(4)	92.780(3)	98.7700(10)
γ, deg	90	90	116.075(4)	90	90
volume, Å^3	2134.2(14)	6693(2)	1140.98(18)	3739.8(6)	4208.38(6)
Z	4	8	2	4	4
density, Mg m^{-3}	1.833	1.513	1.561	1.533	1.528
abs coeff, mm^{-1}	0.770	0.360	0.677	0.400	0.486
F(000)	1168	3120	548	1752	1960
cryst size, mm	0.05 × 0.06 × 0.16	0.55 × 0.60 × 0.70	0.12 × 0.27 × 0.70	0.18 × 0.35 × 0.55	0.07 × 0.09 × 0.25
θ range, deg	2.76 to 26.49	2.4 to 27.25	2.26 to 27.43	2.43 to 27.55	2.5 to 25.74
limiting indices	$-14 \le h \le 14, -16 \le k \le 16, -16 \le l \le 16$	$-25 \le h \le 25, -21 \le k \le 16, -26 \le l \le 26$	$-13 \le h \le 13, -14 \le k \le 14, -18 \le l \le 18$	$-11 \le h \le 5, -15 \le k \le 15, -42 \le l \le 43$	$-14 \le h \le 14, -11 \le k \le 19, -31 \le l \le 32$
reflns collected	18 411	72 912	22 572	24 893	45 695
reflns unique [$I > 2\sigma(I)$]	4385 (3204)	15 161 (11 450)	5146 (4451)	8531 (7106)	9605 (6430)
data/restraints/ params	4385/0/298	15 161/0 /883	5146/0/283	8531/0/505	9605/0/613
goodness-of-fit on F^2	1.002	1.039	1.043	1.141	1.013
R_1 [$I > 2\sigma(I)$] (all data)	0.0458 (0.0756)	0.0429 (0.0641)	0.0304 (0.0375)	0.0642 (0.079)	0.0459 (0.0863)
wR_2 [$I > 2\sigma(I)$] (all data)	0.1031 (0.1147)	0.0974 (0.1074)	0.0722 (0.0755)	0.1346 (0.141)	0.0819 (0.0943)
largest diff, e A^{-3}	0.520 and −0.361	0.347 and −0.512	0.368 and −0.425	0.707 and −0.653	0.677 and −0.352

	7a	**7b**	**7d**	**8a**	**11**
empirical formula	$C_{38}H_{34}F_{12}N_2O_2Zr\cdot 2(CH_2Cl_2)$	$C_{48}H_{38}F_{12}N_2O_2Zr\cdot 1.5(C_7H_8)$	$C_{38}H_{24}F_{22}N_2O_2Zr$	$C_{38}H_{34}F_{12}HfN_2O_2\cdot 2(C_7H_8)$	$C_{36}H_{14}F_{33}N_3O_3Zr$
fw	1039.74	1132.23	1049.81	1141.43	1254.72
cryst syst	monoclinic	triclinic	monoclinic	monoclinic	monoclinic
space group	*C*2/*c*	$P\bar{1}$	$P2_1/n$	*C*2/*c*	$P2_1/a$
a, Å	19.4235(16)	9.12390(8)	10.1292(5)	27.555(2)	18.6550(13)
b, Å	12.3987(13)	11.97510(10)	19.7931(9)	12.0391(10)	11.5244(10)
c, Å	18.8797(18)	24.35250(16)	19.9920(9)	17.9936(14)	22.4943(19)
α, deg	90	96.3176(4)	90	90	90
β, deg	109.048(3)	96.7064(5)	102.105(2)	127.787(2)	22.4943(19)
γ, deg	90	100.2415(5)	90	90	90
volume, Å^3	4297.8(7)	2577.04(7)	3919.0(3)	4717.4(6)	4461.7(6)
Z	4	2	4	4	4
density, Mg m^{-3}	1.607	1.459	1.779	1.607	1.868
abs coeff, mm^{-1}	0.595	0.302	0.425	2.302	0.426
F(000)	2096	1158	2080	2288	2448
cryst size, mm	0.20 × 0.20 × 0.20	0.04 × 0.20 × 0.25	0.25 × 0.30 × 0.30	0.26 × 0.37 × 0.44	0.04 × 0.20 × 0.20
θ range, deg	3.29 to 27.4	2.55 to 27.59	2.8 to 27.53	2.73 to 27.52	2.57 to 27.60
limiting indices	$-23 \le h \le 22, -15 \le k \le 11, -14 \le l \le 24$	$-11 \le h \le 11, -15 \le k \le 16, -27 \le l \le 31$	$-13 \le h \le 13, -25 \le k \le 25, -25 \le l \le 22$	$-35 \le h \le 35, -15 \le k \le 15, -22 \le l \le 23$	$-23 \le h \le 22, -14 \le k \le 14, -29 \le l \le 29$
reflns collected	8203	22 178	38 611	35 640	84 939
reflns unique [$I > 2\sigma(I)$]	4230 (3502)	11 757 (6543)	8952 (7468)	5407 (5298)	10 190 (7995)
data/restraints/ params	4230/0/276	11 757/0/687	8952/0/586	5407/0/313	10 190/0/685
goodness-of-fit on F^2	1.055	1.041	1.041	1.049	1.071
R_1 [$I > 2\sigma(I)$] (all data)	0.0337 (0.0445)	0.0852 (0.1587)	0.0285 (0.0387)	0.0154 (0.0159)	0.0713 (0.0852)
wR_2 [$I > 2\sigma(I)$] (all data)	0.0762 (0.0811)	0.2043 (0.2403)	0.0691 (0.0742)	0.0386 (0.0389)	0.2059 (0.2115)
largest diff, e A^{-3}	0.476 and −0.478	3.035 and −0.917	0.573 and −0.41	0.44 and −0.689	1.894 and −0.884

and the two benzyl groups at the axial positions, which is a type **D** structure (Figure 3). This generates a global C_{2v}-symmetric environment around the metal center, and a crystallographic inversion center is actually observed in **7a** and **8a**. The Zr−O (2.001(4)−2.016(2) Å) and Zr−N (2.436(2)−2.483(4) Å) bond distances compare well with those observed in Zr(IV)-Salen[23b,27] (1.962−2.030 and 2.359−2.425 Å, respectively) and Zr(IV) bis(phenoxyimine) compounds (1.964−2.022 and 2.316−2.391 Å, respectively),[8k,23a,28] as well as in the related fluorous dialkoxide-*diamino* complex $\{CH_2NMeCH_2C(CF_3)_2O\}_2Zr(CH_2Ph)_2$.[4a] The Zr−C bonds in this latter complex (2.266(1)−2.271(1) Å)[4a] are just slightly

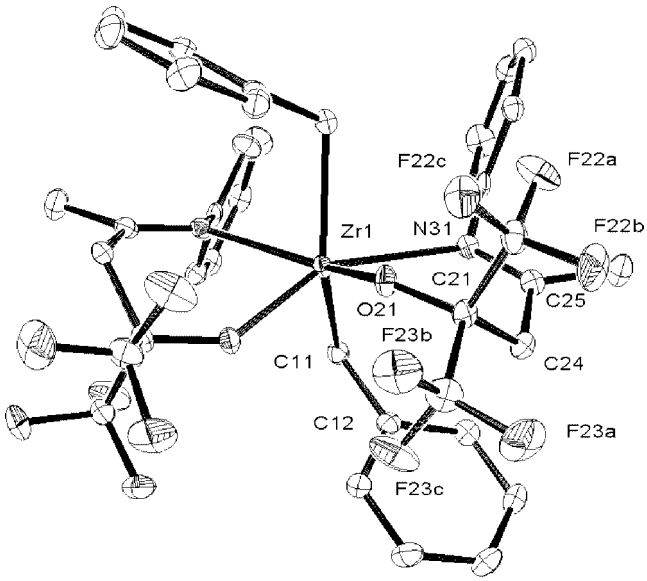

Figure 8. ORTEP view of $Zr(CH_2Ph)_2\{ON^{Me,Ph}\}_2$ (**7a**) (ellipsoids drawn at the 50% probability level; all hydrogen atoms have been omitted for the sake of clarity; Zr(1) is an inversion center and atoms obtained by this symmetry operation are named hereafter with "#"). Selected bond lengths (Å) and angles (deg): Zr(1)−O(21), 2.0163(15); Zr(1)−C(11), 2.310(2); Zr(1)−N(31), 2.4360(18); O(21)#1−Zr(1)−O(21), 86.83(9); O(21)−Zr(1)−C(11)#1, 91.01(7); O(21)−Zr(1)−C(11), 123.51(7); C(11)#1−Zr(1)−C(11), 133.81(12); O(21)#1−Zr(1)−N(31), 149.24(6); O(21)−Zr(1)−N(31), 75.43(6); C(11)#1−Zr(1)−N(31), 82.37(7); C(11)−Zr(1)−N(31), 78.74(7); N(31)−Zr(1)−N(31)#1, 130.55(9); C(12)−C(11)−Zr(1), 109.07-(14).

shorter than those observed in **7a** and **7b** (2.297(6)−2.310(2) Å). Both the benzyl ligands in **7a** and **7b** have a normal structure (C(12)−C(11)−Zr(1), 109.0(4)−111.0(4)°; Zr(1)···C(12), 3.128−3.349 Å), indicative of no significant Zr···Ph interaction. Overall, **7a**, **7b**, and **8a** are best described as 16-electron species, counting the alkoxides as four-electron (σ, π) donors.[4a]

The most stable dibenzyl complexes could also be characterized in solution by NMR techniques. All ^{1}H and ^{19}F NMR data of the complexes **7a**,**b** and **8a** (as well as ^{13}C NMR for **7a**) in toluene-d_8 or CD_2Cl_2 indicate the presence of a single highly symmetric species on the NMR time scale. In each case, a single

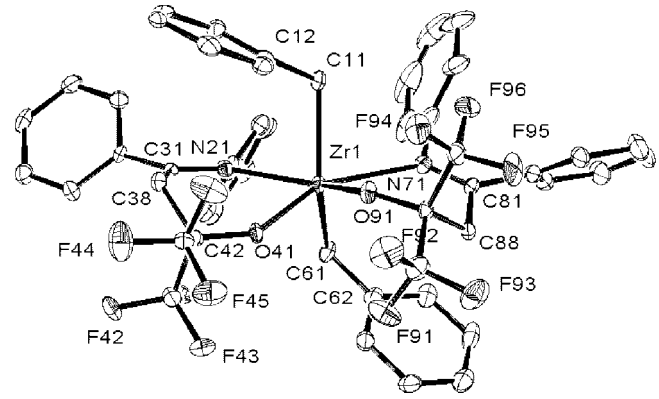

Figure 9. ORTEP view of $Zr(CH_2Ph)_2\{ON^{Ph,Ph}\}_2$ (**7b**) (ellipsoids drawn at the 50% probability level; all hydrogen atoms have been omitted for the sake of clarity). Selected bond lengths (Å) and angles (deg): Zr(1)−O(91), 2.001(4); Zr(1)−O(41), 2.006(4); Zr(1)−C(61), 2.297(6); Zr(1)−C(11), 2.305(6); Zr(1)−N(21), 2.462(5); Zr(1)−N(71), 2.483(4); O(91)−Zr(1)−O(41), 83.31(16); O(91)−Zr(1)−C(61), 121.2(2); O(41)−Zr(1)−C(61), 95.4(2); O(91)−Zr(1)−C(11), 93.9(2); O(41)−Zr(1)−C(11), 120.89(19); C(61)−Zr(1)−C(11), 132.9(2); O(91)−Zr(1)−N(21), 151.67(16); O(41)−Zr(1)−N(21), 75.17(16); C(61)−Zr(1)−N(21), 79.63(19); C(11)−Zr(1)−N(21), 81.91(19); O(91)−Zr(1)−N(71), 74.33(16); O(41)−Zr(1)−N(71), 150.80(17); C(61)−Zr(1)−N(71), 80.90(19); C(11)−Zr(1)−N(71), 79.83(18); N(21)−Zr(1)−N(71), 131.52(16); C(12)−C(11)−Zr(1), 109.0(4); C(62)−C(61)−Zr(1), 111.0(4).

sharp singlet resonance is observed in the ^{19}F{^{1}H} NMR spectrum, and the $CH_2C{=}N$ and M-CH_2 hydrogens appear as singlets in the ^{1}H spectrum. These features are consistent with the C_{2v}-symmetric structures observed in the solid state being retained in solution.[17]

In the absence of suitable crystals for X-ray diffraction, the identity and structure of decomposition products **9a**−**c** and **10a**,**b** were established on the basis of elemental analysis and NMR spectroscopy. Key data include four quartets in the ^{19}F NMR spectra for the nonequivalent CF_3 groups. In the ^{1}H spectra, two doublets of an AB spin pattern are observed for both the diastereotopic C*HH*-Ph and $(CF_3)_2CCHH$ units of the "unaffected" ligand backbone, while the $R^{1C}{=}CH$ of the "affected" ligand appears as a distinctive singlet at δ 4.51−5.29 ppm (CD_2Cl_2, toluene-d_8).[24] ^{13}C NMR data confirm these features.

As for the systems discussed above, reaction of $\{ON^{Me,ArF}\}H$ with $Zr(CH_2Ph)_4$ at −30 °C afforded $Zr(CH_2Ph)_2\{ON^{Me,ArF}\}_2$ (**7d**) (Scheme 6). Crystals of this compound suitable for X-ray diffraction could be isolated at low temperature. In contrast with **7a**, **7b**, and **8a**, the solid-state structure of **7d** features a Zr center in a distorted octahedral geometry, with approximate (noncrystallographic) C_2-symmetry, in which the nitrogen ligand atoms, oxygen ligand atoms, and benzyl groups are arranged in a *cis,trans,cis* fashion (Figure 11), which is a type **F** structure (Figure 3). The Zr−N bond distances in **7d** (2.523(1)−2.552(1)

(25) To prevent this decomposition pathway, the use of *gem*-dimethyl-substituted pro-ligand analogues was attempted. Surprisingly, fluorous (di)imino-(di)ols such as $HOC(CF_3)_2CMe_2C(iPr){=}N(iPr)$ and $[HOC(CF_3)_2CMe_2C(iPr){=}NCH_2-]_2$ were found not to react with $M(CH_2Ph)_4$ (M = Ti, Zr, Hf) in toluene up to 60−80 °C, temperatures at which the latter precursors start decomposing at a significant rate. Reasons for this absence of reactivity, while no obvious steric and electronic effects can be accounted for, remain obscure. To date, such *gem*-dimethyl-substituted pro-ligands could be installed only at aluminum centers, under conditions much more drastic than those used for the parent nonsubstituted pro-ligands; see ref 11.

(26) The reactions of $Zr(CH_2Ph)_4$ with 1 equiv of $\{ON^{Me,Ph}\}H$ or $\{ON^{Ph,Ph}\}H$ were attempted to potentially access the corresponding $Zr(CH_2Ph)_2\{ON^{-R1,R2}\}$ complexes. However, in both cases, NMR monitoring showed that these reactions led to ca. 1:1 mixtures of $Zr(CH_2Ph)_4$ and $Zr(CH_2Ph)_2\{ON^{R1,R2}\}_2$, which further evolve by decomposition of the latter species into $Zr(CH_2Ph)\{ON^{-R1,R2}\}\{ON^{R1,R2}\}$. Those observations indicate that disproportionation of the putative intermediate species $[Zr(CH_2Ph)_3\{ON^{R1,R2}\}]$ or consecutive reaction of the latter species with $\{ON^{Ph,Ph}\}H$ (to form in both cases $Zr(CH_2Ph)_2\{ON^{R1,R2}\}_2$) is faster than abstraction of a hydrogen atom from the ligand backbone.

(27) Clarkson, G. J.; Gibson, V. C.; Goh, P. K. Y.; Hammond, M. L.; Knight, P. D.; Scott, P.; Smit, T. M.; White, A. J. P.; Williams, D. J. *Dalton Trans.* **2006**, 5484.

(28) (a) Ivanchev, S. S.; Truno, V. A.; Rybakov, V. B.; Al'bov, D. V.; Rogozin, D. G. *Dokl. Akad. Nauk. SSSR* **2005**, *404*, 57. (b) Strauch, J.; Warren, T. H.; Erker, G.; Frohlich, R.; Saarenketo, P. *Inorg. Chim. Acta* **2000**, *300*, 810. (c) Said, M.; Hughes, D. L.; Bochmann, M. *Inorg. Chim. Acta* **2006**, *359*, 3467. (d) Bott, R. K. J.; Hughes, D. L.; Schormann, M.; Bochmann, M.; Lancaster, S. J. *J. Organomet. Chem.* **2005**, *665*, 135. (e) Lamberti, M.; Gliubizzi, R.; Mazzeo, M.; Tedesco, C.; Pellecchia, C. *Macromolecules* **2004**, *37*, 276. (f) Marsh, R. E. *Acta Crystallogr., Sect. B: Struct. Sci.* **2004**, *60*, 252. (g) Chen, S.; Zhang, X.; Ma, H.; Lu, Y.; Zhang, Z.; Li, H.; Lu, Z.; Cui, N.; Hu, Y. *J. Organomet. Chem.* **2005**, *690*, 4184. (h) Woodman, P. R.; Munslow, I. J.; Hitchcock, P. B.; Scott, P. *J. Chem. Soc., Dalton Trans.* **1999**, 4069. (i) Woodman, P.; Hitchcock, P. B.; Scott, P. *Chem. Commun.* **1996**, 2735.

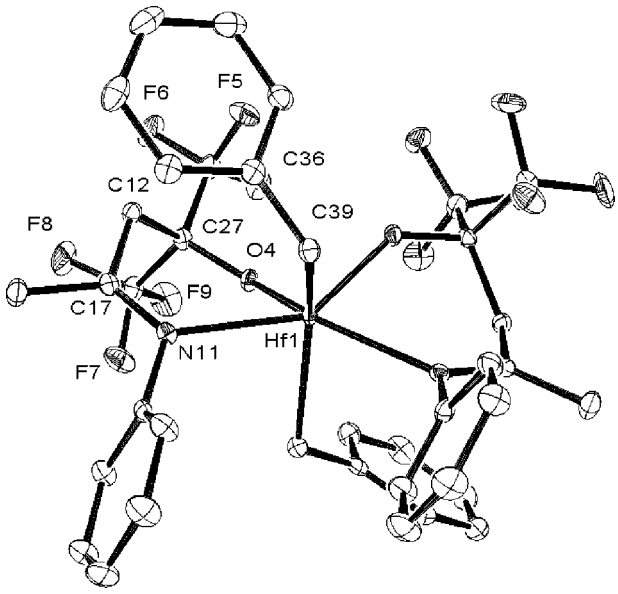

Figure 10. ORTEP view of $Hf(CH_2Ph)_2\{ON^{Me,Ph}\}_2$ (**8a**) (ellipsoids drawn at the 50% probability level; all hydrogen atoms have been omitted for the sake of clarity; Hf(1) is an inversion center and atoms obtained by this symmetry operation are named hereafter with "#"). Selected bond lengths (Å) and angles (deg): N(11)−Hf(1), 2.3795(12); O(4)−Hf(1), 2.0100(10); C(39)−Hf(1), 2.2951(14); O(4)−Hf(1)−O(4)#1, 84.01(6); O(4)−Hf(1)−C(39), 126.42(5); O(4)#1−Hf(1)−C(39), 89.56(5); C(39)−Hf(1)−C(39)#1, 133.55(8); O(4)−Hf(1)−N(11), 76.33(4); O(4)#1−Hf(1)−N(11), 144.37(4); C(39)−Hf(1)−N(11), 79.08(5); C(39)#1−Hf(1)−N(11), 83.31(5); N(11)−Hf(1)−N(11)#1, 134.35(6); C(36)−C(39)−Hf(1), 113.14(10).

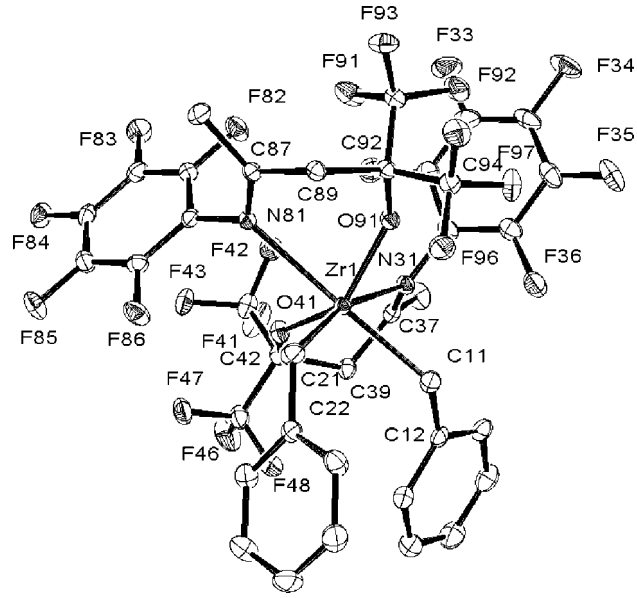

Figure 11. ORTEP view of $Zr(CH_2Ph)_2\{ON^{Me,ArF}\}_2$ (**7d**) (ellipsoids drawn at the 50% probability level; all hydrogen atoms have been omitted for the sake of clarity). Selected bond lengths (Å) and angles (deg): Zr(1)−O(41), 1.9848(12); Zr(1)−O(91), 2.0017(12); Zr(1)−C(21), 2.2927(18); Zr(1)−C(11), 2.3014(18); Zr(1)−N(31), 2.5229(15); Zr(1)−N(81), 2.5515(14); O(41)−Zr(1)−O(91), 135.40(5); O(41)−Zr(1)−C(21), 103.59(6); O(91)−Zr(1)−C(21), 107.43(6); O(41)−Zr(1)−C(11), 115.12(6); O(91)−Zr(1)−C(11), 99.01(6); C(21)−Zr(1)−C(11), 84.81(7); O(41)−Zr(1)−N(31), 76.45(5); O(91)−Zr(1)−N(31), 80.83(5); C(21)−Zr(1)−N(31), 165.78(6); C(11)−Zr(1)−N(31), 82.42(6); O(41)−Zr(1)−N(81), 82.62(5); O(91)−Zr(1)−N(81), 73.70(5); C(21)−Zr(1)−N(81), 77.79(6); C(11)−Zr(1)−N(81), 157.83(6); N(31)−Zr(1)−N(81), 116.08(5); C(12)−C(11)−Zr(1), 119.36(12).

Å) are longer than those in **7a** and **7b** (2.436(2)−2.483(4) Å), which likely reflects the *trans* influence of the benzyl groups. The latter groups are somewhat more bent than in **7a** and **7b** (C(12)−C(11)−Zr(1), 119.36(12)°; C(12)···Zr(1), 3.302 Å). Otherwise, the Zr−O and Zr−C bond distances compare well with those in **7a** and **7b**. On the other hand, the ^1H and ^{19}F NMR data for **7d** in toluene-d_8 solution appear strictly similar to those for **7a**, **7b**, and **8a**; that is, the type **F** structure observed in the solid state is not retained in solution but transformed to a C_{2v}-symmetric structure of type **D**. This observation indicates that coordination of the $\{ON^{R1,R2}\}^-$ fragments onto group 4 metals is rather labile, although it most often leads to the observation of a single species.

Scheme 6

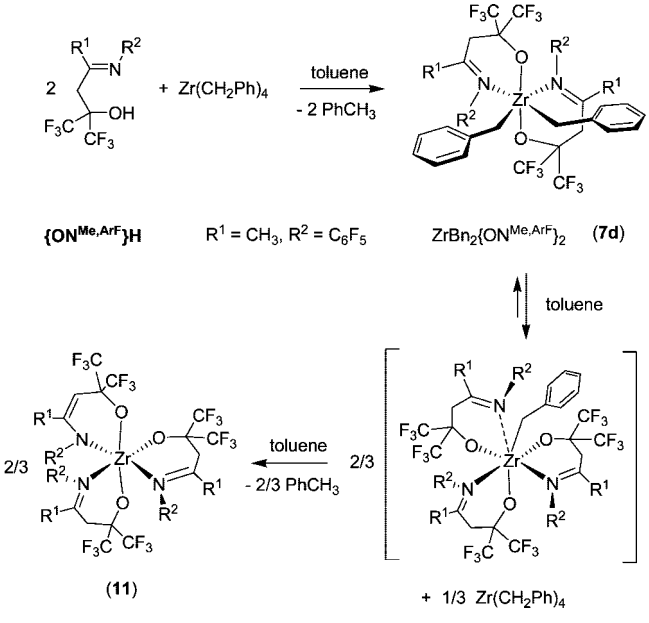

The decomposition pathway of **7d** was found to proceed in a somehow different way than for **7a**, **7b**, and **8a**. When a toluene solution of **7d** was kept at room temperature, complete decomposition took place within a few hours, leaving colorless crystals of $Zr\{ON^{Me,ArF}\}_2\{ON^{-Me,ArF}\}$ (**11**) (Scheme 6). An X-ray diffraction study and multinuclear NMR spectroscopy of these crystals indicated that there is no more benzyl group in this compound, but three $\{ON^{Me,ArF}\}$ ligand units including one ($\{ON^{-Me,ArF}\}$) that acts as an α,β-unsaturated amido-alkoxy dianionic moiety. We can reasonably assume that compound **11** arises from a ligand redistribution in **7d**, to generate a transient intermediate $Zr(CH_2Ph)\{ON^{Me,ArF}\}_3$ (not observed by NMR), which further undergoes rapid abstraction of a hydrogen from the methylene ligand backbone by the benzyl group (Scheme 6).

The X-ray diffraction study of **11** revealed a mononuclear structure with the Zr center in a slightly distorted octahedral environment (Figure 12). As a result of the formation of an amido ligand, the Zr−N bond in the "affected" ligand unit (2.179(4) Å) is significantly shorter than the two other Zr−N(imino) bond distances (2.378(5)−2.393(5) Å), while the Zr−O bond distances are essentially all identical to those observed in **7a**,**b**,**d**. The ^1H and ^{19}F NMR data for **11** in benzene-d_6 show expectedly two sets of resonances in a 2:1 ratio for the

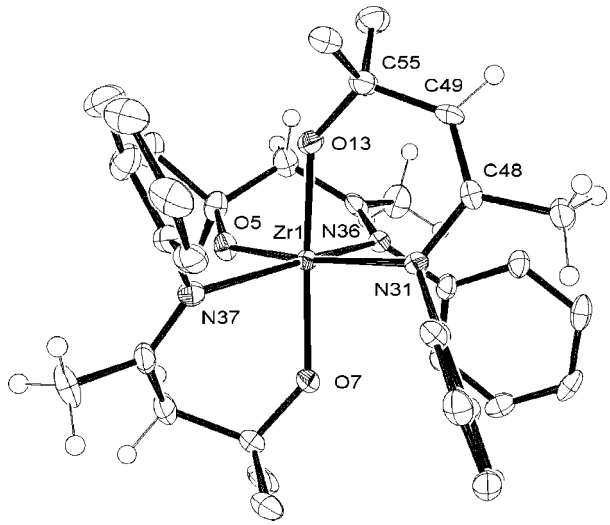

Figure 12. ORTEP view of $Zr\{ON^{Me,ArF}\}_2\{ON^{-Me,ArF}\}$ (**11**) (ellipsoids drawn at the 50% probability level; all fluorine atoms have been omitted for the sake of clarity). Selected bond lengths (Å) and angles (deg): Zr(1)−O(13), 1.999(4); Zr(1)−O(7), 2.011(4); Zr(1)−O(5), 2.016(4); Zr(1)−N(31), 2.179(4); Zr(1)−N(36), 2.378(5); Zr(1)−N(37), 2.393(5); O(13)−C(55), 1.371(7); C(49)−C(55), 1.508(8); C(48)−C(49), 1.344(8); N(31)−C(48), 1.416(7); O(13)−Zr(1)−O(7), 166.46(16); O(13)−Zr(1)−O(5), 94.49(16); O(7)−Zr(1)−O(5), 96.73(16); O(13)−Zr(1)−N(31), 81.63(16); O(7)−Zr(1)−N(31), 88.54(16); O(5)−Zr(1)−N(31), 169.58(16); O(13)−Zr(1)−N(36), 92.85(16); O(7)−Zr(1)−N(36), 97.08(15); O(5)−Zr(1)−N(36), 76.76(15); N(31)−Zr(1)−N(36), 93.71(16); O(13)−Zr(1)−N(37), 95.61(16); O(7)−Zr(1)−N(37), 77.84(15); O(5)−Zr(1)−N(37), 85.19(15); N(31)−Zr(1)−N(37), 104.76(16); N(36)−Zr(1)−N(37), 160.60(16).

two "unaffected" and the "affected" ligand units, respectively (see Experimental Section).

Dichloride Complexes of Zirconium. Efforts have also been made to access dichlorozirconium complexes, potentially useful for polymerization catalysis. $ZrCl_2\{ON^{Me,Ph}\}_2$ (**12a**) and $ZrCl_2\{ON^{Ph,Ph}\}_2$ (**12b**) could be obtained in moderate yields, in a one-pot procedure, by generating first "$Zr(n\text{Bu})_2Cl_2$" from $ZrCl_4$ and nBuLi[29] and then adding 2 equiv of the corresponding pro-ligand $\{ON^{R1,R2}\}H$ to perform an alkane elimination (Scheme 7).[4a,30] Both compounds are moderately soluble in aromatic solvents (toluene, benzene) and sparingly soluble in aliphatic hydrocarbons (hexanes). NMR data in benzene-d_6 of the crude products recovered following this procedure showed that these are mixtures of a C_{2v}-symmetric and a C_1-symmetric isomer (**12a**, 70:30; **12b**, 30:70). When heated above 60 °C in benzene-d_6, these (kinetic) mixtures slowly isomerize to yield the C_{2v}-symmetric (thermodynamic) isomer. Also, C_1-**12a**,**b** proved to be much less soluble than C_{2v}-**12a**,**b** and could be selectively isolated by washing the (kinetic) crude mixtures with hot hexanes (see Experimental Section). C_{2v}-**12a**,**b** show the same NMR features as those discussed above for complexes **3**, **7**, and **8**. The C_1-symmetric isomers of **12a**,**b** are characterized by four quartets of equal intensity in the ^{19}F NMR spectrum (these quartets are broadened and two of them overlap in the case of **12b**) and a complete set of resonances for each individual nonaromatic hydrogen in the ^1H NMR spectrum.

Scheme 7

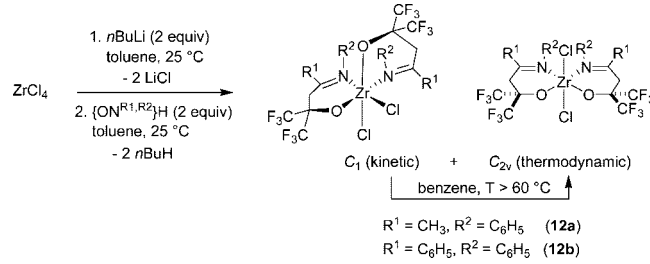

Repeated attempts under various conditions to obtain such complexes by regular salt metathesis of $ZrCl_4$ (or $ZrCl_4(THF)_2$) with the Li^+ (*in situ*-generated), Na^+, or K^+ (isolated; see Experimental Section) salt of $\{ON^{Me,Ph}\}^-$ and $\{ON^{Ph,Ph}\}^-$ led to intractable mixtures of compounds that could not be separated nor unambiguously identified.[20] A similar approach from $\{ON^{Me,ArF}\}Li$ (*in situ* generated) or $\{ON^{Me,ArF}\}K$ (isolated; see Experimental Section) afforded $ZrCl_2\{ON^{Me,ArF}\}_2$ (**12c**) in poor yield, but this compound features so poor solubility in all common organic solvents that it could be authenticated only on the basis of microanalysis.

Ethylene Polymerization. The complexes based on bidentate ligands were briefly investigated in ethylene polymerization.[31] Neutral isopropoxide and chloride complexes were activated with MAO or a combination of $[Ph_3C][B(C_6F_5)_4]$ and $Al(i\text{Bu})_3$,[32] while $[Ph_3C][B(C_6F_5)_4]$ was used to generate *in situ* cationic benzyl-hafnium species from the relatively stable dibenzyl complex **8a**. The results are summarized in Table 2.

Two general characteristics can be drawn from these preliminary investigations. First, all systems show relatively high activity in the early stages of the polymerizations but rapidly deactivate over a 0.1−10 min time period, after which no ethylene uptake is noticed.[33] In fact, in some cases, all of the polyethylene is formed within the first 10 s of the experiment. As a consequence, the activity data reported in Table 2, which were calculated over the whole 10 min time period of the experiments, barely reflect the real behavior of the catalyst systems. These apparent activities, which are usually in the range 100−200 kg PE mol^{-1} h^{-1}, no matter the nature of the metal and ligand, are of the same order of magnitude as those reported for related catalysts based on discrete zirconium precursors having amino-alkoxide or amino-dialkoxide ligands[34] and somewhat lower than those observed for systems based on sulfur-bridged dialkoxide ligands,[30,35] although direct comparisons are difficult due to differences in polymerization time and conditions.

High initial activities and fast deactivation in ethylene polymerizations have been also reported with group 4 metal catalysts supported by sulfur-bridged dialkoxide $\{OSO\}^{2-}$ ligands.[30] In this case, ligand transfer between group 4 metal

(29) (a) Eisch, J. J.; Owuor, F. A.; Shi, X. *Organometallics* **1999**, *18*, 1583. (b) Eisch, J. J.; Owuor, F. A.; Otieno, P. O. *Organometallics* **2001**, *20*, 4132.

(30) Lavanant, L.; Silvestru, A.; Faucheux, A.; Toupet, L.; Jordan, R. F.; Carpentier, J.-F. *Organometallics* **2005**, *24*, 5604.

(31) Complexes **1** and **2** were also briefly investigated in polymerization catalysis, although no valuable performance was expected, considering the equatorial coordination of the tetradentate ligand and the anticipated absence of *cis* vacant sites in the resulting cationic species. As a matter of fact, for instance, when complex **1** was activated with MAO (1000 equiv, toluene solution), no polymerization activity was observed (1 atm ethylene, 25 °C).

(32) (a) Chien, J. C. W.; Xu, B. *Makromol. Chem. Rapid Commun.* **1993**, *14*, 109. (b) Chien, J. C. W.; Tsai, W. M. *Makromol. Chem. Macromol. Symp.* **1993**, *66*, 141. (c) Chen, Y. X.; Rausch, M. D.; Chien, J. C. W. *Organometallics* **1994**, *13*, 748. (d) Chien, J. C. W.; Rausch, M. D. *J. Polym. Sci. Part A: Polym. Chem.* **1994**, *32*, 2387. (e) Song, F. S.; Cannon, R. D.; Lancaster, S. J.; Bochmann, M. *J. Mol. Catal. A* **2004**, *218*, 21.

(33) In these experiments, polyethylene was recovered in virtually the same amount as that of ethylene consumed; oligomers (if any) were therefore negligible.

Table 2. Ethylene Polymerization Data[a]

entry	catalyst precursor	activator/scavenger (equiv vs metal)	yield (g)	activity[b] (kg PE mol^{-1} h^{-1})	M_w[c] (10^3 g mol^{-1})	M_w/M_n[c]	T_m[d] (°C)
1	Ti(O*i*Pr)$_2${ON^{Me,Ph}}$_2$ (**3a**)	MAO (1500)	0.429	195	insoluble[e]		135
2	Ti(O*i*Pr)$_2${ON^{Ph,Ph}}$_2$ (**3b**)	MAO (1450)	0.344	174	427	2.7	136
3	TiCl$_2$(O*i*Pr){ON^{Me,Ph}} (**4**)	MAO (1100)	0.476	201	399	4.7	137
4	TiCl(O*i*Pr){ON^{Ph,Ph}}$_2$ (**5/6**)[f]	MAO (1250)	0.460	222	375	4.4	136
5	ZrCl$_2${ON^{Me,Ph}}$_2$ (**12a**)	MAO (1350)	0.387	159	680	8.2	140
6	ZrCl$_2${ON^{Ph,Ph}}$_2$ (**12b**)	MAO (1200)	0.285	132	insoluble[e]		133
7	ZrCl$_2${ON^{Ph,Ph}}$_2$ (**12b**)	[Ph$_3$C][B(C$_6$F$_5$)$_4$] (3)/Al(*i*Bu)$_3$ (40)	0.009	4	insoluble[e]		133
8	ZrCl$_2${ON^{Me,ArF}}$_2$ (**12c**)	MAO (1300)	0.430	213	insoluble[e]		141
9	ZrCl$_2${ON^{Me,ArF}}$_2$ (**12c**)	[Ph$_3$C][B(C$_6$F$_5$)$_4$] (2)/Al(*i*Bu)$_3$ (100)	0.520	99	insoluble[e]		144
10	Hf(CH$_2$Ph)$_2${ON^{Me,Ph}}$_2$ (**8a**)	[Ph$_3$C][B(C$_6$F$_5$)$_4$] (2.2)/Al(*i*Bu)$_3$ (48)	0	0			

[a] Unless otherwise stated, all polymerization experiments were conducted at 50 °C under 7−8 atm of ethylene for 10 min, using 12−32 μmol of catalyst precursor in 50−60 mL of toluene; the results shown for each entry are representative of at least two reproducible runs. [b] Average activity calculated over the whole polymerization time (10 min). [c] Determined by GPC in 1,2,4-trichlorobenzene at 150 °C. [d] Determined by DSC (first heating). [e] PE could not be solubilized in 1,2,4-trichlorobenzene at 160 °C. [f] A mixture of complexes **5** and **6** was used.

Scheme 8. Proposed Deactivation Pathway in Ethylene Polymerizations Catalyzed by M-{ON^{R1,R2}}/Activator Systems (P stands for the growing polyethylenyl chain)

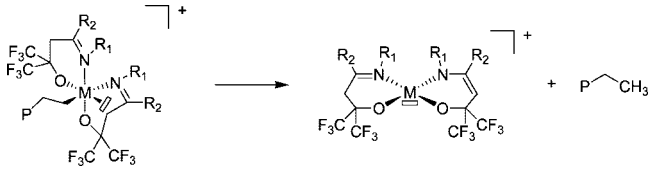

and Al centers was suggested as a possible origin of the catalyst decay. No direct evidence could be found for such a process in the present M-{ON^{R1,R2}}/MAO systems.[36] The similar catalyst behavior (decay) observed with quite different activators (MAO[37] vs [Ph$_3$C][B(C$_6$F$_5$)$_4$] with Al(*i*Bu)$_3$; compare entries 8 and 9, Table 2) suggests that another deactivation pathway may be operative in the present systems. Based on the aforementioned observation of hydrogen abstraction by a benzyl group in neutral Zr(CH$_2$Ph)$_2${ON^{R1,R2}}$_2$ species (*vide supra*), we assume that a similar process may take place in related cationic species (Scheme 8). Hydrogen abstraction from the ligand backbone by the growing polyethylenyl chain would eventually result in the formation of an alkyl-free, inactive species. In this regard, it is noteworthy that no polymerization at all was noticed when dibenzyl complex **8a** was used as the catalyst precursor (Table 2, entry 10).

The second general feature of these polymerizations concerns the nature of the polymers obtained. All the polyethylenes produced with the [M-{ON^{R1,R2}}] systems under the conditions used have a melting temperature in the range 133−144 °C, indicative of essentially linear long-chain microstructures. The few polymers that proved to be soluble in 1,2,4-trichlorobenzene at 160 °C (and thus analyzable by GPC) showed high molecular weight. Many polyethylenes could not be solubilized, calling for even higher molecular weights. Polyethylenes that could be analyzed by GPC had broad molecular weight distributions, although most of them feature monomodal shapes with long tailing on low[33] and high molecular weights (see the Supporting Information).

Conclusions

The preparation of discrete group 4 metal complexes based on Schiff base bi- and tetradentate fluorous (di)imino-(di)alkoxide ligands {ON^{R1,R2}}$^-$ and {ON^{Et}NO}$^{2-}$ has been studied. Diisopropoxide-Ti(IV) and dibenzyl-Zr(IV) and -Hf(IV) complexes have been obtained using straightforward procedures; the preparation of dichloride-Ti(IV) and -Zr(IV) complexes based on bidentate ligands proved to be somewhat more difficult. Despite the flexibility of the {ON^{R1,R2}}$^-$ and {ON^{Et}NO}$^{2-}$ ligands (the bis(trifluoromethyl)alkoxide is not conjugated with the imino group, in contrast to phenoxy-imine and salen ligands) and the lability of their coordination onto group 4 metals (two different stereoisomers of a given compound are sometimes observed in the solid state and in solution), the formation of a single stereoisomer is most often observed, usually with equatorial coordination of the (di)imino-(di)alkoxide functions. This coordination behavior contrasts with that adopted by related fluorous di*amino*-dialkoxide ligands [helicoidal wrapping of the ligand around the metal center, with both alkoxides located at apical positions, which is a type **B** structure].[4a] This confirms that imino groups reduce flexibility of the ligand framework.

Another interesting feature revealed in this study is the rapid decomposition of dibenzyl-Zr(IV) and -Hf(IV) complexes, via abstraction of a hydrogen from the ligand framework by a benzyl group. This phenomenon, which is observed only for M(CH$_2$Ph)$_2${ON^{R1,R2}}$_2$ complexes based on bidentate ligands, while Zr(CH$_2$Ph)$_2${ON^{Et}NO} is stable, provides a reasonable rational basis for the observed rapid deactivation of putative [M(alkyl){ON^{R1,R2}}$_2$]$^+$ catalytic species during ethylene polymerization.

The many possibilities to tune such fluorous (di)alkoxide-(di)imino ligands[5] open avenues for designing and preparing new series of group 4 metal complexes. Results of ongoing studies on the coordination chemistry of these original ligands with oxophilic metal centers, the origin of deactivation pathways, and the application of these discrete complexes in catalysis will be reported in due course.

Experimental Section

General Procedures. All experiments were carried out under purified argon using standard Schlenk techniques or in a glovebox.

(34) Zr(CH$_2$Ph)$_2$[RN{CH$_2$CH$_2$C(O)R′$_2$}$_2$]/MAO (1:500) gave at 50 °C, 5 atm, 136−384 kg PE mol^{-1} h^{-1} with M_w = 143−452,000, M_w/M_n = 3.4−5.7; see: (a) Shao, P.; Gendron, R. A. L.; Berg, D. J.; Bushnell, G. W. *Organometallics* **2000**, *19*, 509–520. (b) Zr(CH$_2$Ph)$_2${PyC(CF$_3$)$_2$O}$_2$/MAO (1:1000) gave at 30 °C, 8 atm, 10 kg PE mol^{-1} h^{-1} with M_w = 375 000, M_w/M_n = 28; Zr(CH$_2$Ph)$_2${PyC(CF$_3$)$_2$O}$_2$/B(C$_6$F$_5$)$_3$ (1:1) gave at 40 °C, 3 atm, 96 kg PE mol^{-1} h^{-1} with M_w = 16 000, M_w/M_n = 2.6; see ref 3d. (c) Berg and Kress observed insignificant or no ethylene polymerization activity with Zr(CH$_2$Ph)$_2$[RN{CH$_2$CH$_2$C(O)R′$_2$}$_2$]/B(C$_6$F$_5$)$_3$ and Zr(CH$_2$Ph)$_2$(2,6-bis{menthoxo}pyridyl)/B(C$_6$F$_5$)$_3$ combinations, respectively, and attributed it to the formation of tight ion pairs; see ref 34a and: Gauvin, R. M.; Osborn, J. A.; Kress, J. *Organometallics* **2000**, *19*, 2944.

(35) Eisen and co-workers have reported that the TiCl$_2$[Py{CPh$_2$O}$_2$]/MAO combination exhibits modest ethylene polymerization activity (20 °C, 1 atm); see: Mack, H.; Eisen, M. *J. Chem. Soc., Dalton Trans.* **1998**, 917.

(36) For transfer a phenoxyimino ligand from a Zr to Al center: Makio, H.; Fujita, T. *Macromol. Symp.* **2004**, *213*, 221.

Hydrocarbon solvents, diethyl ether, and tetrahydrofuran were distilled from Na/benzophenone; toluene and pentane were distilled from Na/K alloy under nitrogen and degassed by freeze−vacuum−thaw cycles prior to use. Chlorinated solvents were distilled from calcium hydride. Deuterated solvents (>99.5% D, Eurisotop) were freshly distilled from the appropriate drying agent under argon and degassed prior to use. Pro-ligands $\{ON^{Et}NO\}H_2$ and $\{ON^{R1,R2}\}H_2$ were synthesized according to the reported procedures.[5] Zirconium and hafnium precursors $Zr(CH_2Ph)_4$ and $Hf(CH_2Ph)_4$[38] were prepared following literature procedures. $ZrCl_4$, $TiCl_4$, and $Ti(OiPr)_4$ were purchased from Strem Chemicals and used as received. $[Ph_3C][B(C_6F_5)_4]$ (Boulder), $Al(iBu)_3$ (Aldrich), and MAO (30 wt % solution in toluene, Albermale; contains ca. 10 wt % of free $AlMe_3$) were used as received.

NMR spectra were recorded in Teflon-valved NMR tubes on Bruker AC-200, AC-300, and AM-500 spectrometers at 20 °C unless otherwise stated. ^1H and ^{13}C NMR chemical shifts were determined using residual solvent resonances and are reported versus $SiMe_4$. Assignment of signals was made from 2D $^1H-^1H$ COSY and $^1H-^{13}C$ HMQC and HMBC NMR experiments. ^{19}F chemical shifts were determined by external reference to an aqueous solution of $NaBF_4$. All coupling constants are given in hertz. Elemental analyses (C, H, N) were performed using a Flash EA1112 CHNS Thermo Electron apparatus and are the average of two independent determinations.

Reaction of $TiCl_2(OiPr)_2$ with $\{ON^{Et}NO\}H_2$: Synthesis of $TiCl_2\{ON^{Et}NO\}$ (1). A solution of diol $\{ON^{Et}NO\}H_2$ (100 mg, 0.21 mmol) in toluene (4 mL) was added to a solution of $TiCl_4$ (20.1 mg, 0.106 mmol) and $Ti(OiPr)_4$ (30.1 mg, 0.106 mmol) in toluene (4 mL) at −30 °C. The reaction mixture was kept at −30 °C overnight; afterward colorless crystals precipitated. The crystals were separated from the supernatant, washed with a minimal amount of toluene, and dried under vacuum to give **1** as colorless crystals (70 mg, 56%); suitable crystals for X-ray diffraction studies were obtained from this batch. ^1H NMR (500 MHz, CD_2Cl_2, 298 K): δ 2.37 (s, 6H, CH_3), 3.62 (s, 4H, $CH_2C{=}N$), 4.16 (s, 4H, NCH_2). $^{13}C\{^1H\}$ NMR (125 MHz, CD_2Cl_2, 298 K): δ 23.6 (CH_3), 41.8 ($CH_2C{=}N$), 46.7 (NCH_2), 85.3 ($C(CF_3)_2$), 122.2 (q, $^1J_{CF}$ = 285.3, CF_3), 173.9 ($N{=}C(CH_3)$). $^{19}F\{^1H\}$ NMR (188 MHz, CD_2Cl_2, 298 K): δ −76.2 (s, 12F). Anal. Calcd for $C_{14}H_{14}Cl_2F_{12}N_2O_2Ti$: C, 28.55; H, 2.40; N, 4.76. Found: C, 28.9; H, 2.6; N, 4.7.

Reaction of $\{ON^{Et}NO\}H_2$ with $Zr(CH_2Ph)_4$: Synthesis of $Zr(CH_2Ph)_2\{ON^{Et}NO\}$ (2). NMR-scale synthesis: A Teflon-valved NMR tube was charged with diol $\{ON^{Et}NO\}H_2$ (25.7 mg, 54.4 μmol) and $Zr(CH_2Ph)_4$ (24.8 mg, 54.4 μmol), and dry toluene-d_8 (ca. 0.5 mL) was vacuum-transferred in at −78 °C. The tube was kept for 3−4 h at −30 °C, and NMR was recorded at room temperature, revealing the formation of **2** in 95% yield, as determined by ^1H NMR spectroscopy. Preparative synthesis: A solution of $Zr(CH_2Ph)_4$ (0.41 g, 0.89 mmol) in toluene (3 mL) precooled at −30 °C was added under vigorous stirring to a solution of $\{ON^{Et}NO\}H_2$ (0.42 g, 0.86 mmol) in toluene (4 mL) at −30 °C. The reaction mixture was kept at −30 °C overnight, after which **2** precipitated as a yellow crystalline solid, which was separated and dried *in vacuo* (0.25 g, 38%). ^1H NMR (500 MHz, CD_2Cl_2, 298 K): δ 2.09 (s, 4H, CH_2Ph), 2.12 (s, 6H, CH_3), 2.85 (s, 4H, $CH_2C{=}N$), 3.62 (s, 4H, NCH_2), 6.64 (d, $^3J_{HH}$ = 7.5, 4H, *o*-Ph), 6.71 (t, $^3J_{HH}$ = 7.5, 2H, *p*-Ph), 7.00 (m, $^3J_{HH}$ = 7.5, 4H, *m*-Ph). $^{13}C\{^1H\}$ NMR (125 MHz, CD_2Cl_2, 298 K): δ 21.1 (CH_2Ph), 24.0 (CH_3), 40.6 ($CH_2{-}C{=}N$), 51.3 (NCH_2), 79.5 ($C(CF_3)_2$), 119.9 (*p*-Ph), 123.8 (CF_3), 125.5 (*o*-Ph), 127.6 (*m*-Ph), 151.1 (*i*-Ph), 177.5 ($N{=}C(CH_3)$). $^{19}F\{^1H\}$ NMR (188 MHz, CD_2Cl_2, 298 K): δ −76.9 (s, 12F). Anal. Calcd for $C_{28}H_{28}F_{12}N_2O_2Zr$: C, 45.22; H, 3.79; N, 3.77. Found: C, 45.8; H, 3.8; N, 3.7.

Reaction of $\{ON^{Me,Ph}\}H$ with $Ti(OiPr)_4$: Synthesis of $Ti(OiPr)_2\{ON^{Me,Ph}\}_2$ (3a). A solution of $Ti(OiPr)_4$ (0.240 g, 0.844 mmol) in toluene (ca. 2.5 mL) was added dropwise at −25 °C to a solution of $\{ON^{Me,Ph}\}H$ (0.510 g, 1.704 mmol). The mixture was stirred until it reached room temperature, and volatiles were removed under vacuum. The solid residue was washed with cold pentane (ca. 5 mL) and dried under vacuum to give **3a** as a white solid (0.410 g, 63%). Crystals of **3a** suitable for X-ray diffraction studies were obtained by recrystallization from a mixture of toluene and hexane. ^1H NMR (500 MHz, benzene-d_6, 298 K): δ 1.14 (d, $^3J_{HH}$ = 6.1, 12H, $CH(CH_3)_2$), 1.25 (s, 6H, CH_3), 3.10 (s, 4H, CH_2), 4.85 (hept, $^3J_{HH}$ = 6.1, 2H, $CH(CH_3)_2$), 6.53 (d, $^3J_{HH}$ = 7.5, 4H, *o*-Ph), 6.94 (t, $^3J_{HH}$ = 7.2, 2H, *p*-Ph), 7.03 (t, $^3J_{HH}$ = 7.6, 4H, *m*-Ph). $^{13}C\{^1H\}$ NMR (125 MHz, benzene-d_6, 298 K): δ 24.8 (CH_3), 37.9 (CH_2), 80.2 (CH), 81.5 (hept, $^2J_{CF}$ = 28.0, $C(CF_3)_2$), 122.4 (*o*-Ph), 124.5 (q, $^1J_{CF}$ = 293.0, CF_3), 125.1 (*p*-Ph), 128.3 (*m*-Ph), 150.1 (*i*-Ph), 175.6 (C=N). $^{19}F\{^1H\}$ NMR (188 MHz, benzene-d_6, 298 K): δ −76.6 (s, 12F). Anal. Calcd for $C_{30}H_{34}F_{12}N_2O_4Ti$: C, 47.26; H, 4.49; N, 3.67. Found: C, 47.2; H, 4.6; N, 3.7.

Reaction of $\{ON^{Ph,Ph}\}H$ with $Ti(OiPr)_4$: Synthesis of $Ti(OiPr)_2\{ON^{Ph,Ph}\}_2$ (3b). This compound was prepared following a similar procedure to the one described above for **3a**, starting from $Ti(OiPr)_4$ (34.9 mg, 122.8 μmol) and $\{ON^{Ph,Ph}\}H$ (88.7 mg, 245.5 μmol). Compound **3b** was obtained as a pale yellow solid (70.0 mg, 64%). ^1H NMR (300 MHz, benzene-d_6, 298 K): δ 1.24 (d, $^4J_{HH}$ = 6.1, 12H, $CH(CH_3)_2$), 3.70 (s, 4H, CH_2), 5.00 (hept, $^3J_{HH}$ = 6.1, 2H, $CH(CH_3)_2$), 6.71−6.85 (m, 20H, Ph). ^1H NMR (300 MHz, CD_2Cl_2, 298 K): δ 1.06 (d, $^4J_{HH}$ = 6.0, 12H, $CH(CH_3)_2$), 3.55 (s, 4H, CH_2), 4.75 (hept, $^3J_{HH}$ = 6.0, 2H, $CH(CH_3)_2$), 6.67−7.31 (m, 20H, Ph). $^{13}C\{^1H\}$ NMR (75 MHz, benzene-d_6, 298 K): δ 24.9 ($CH(CH_3)_2$), 39.2 (CH_2), 80.7 ($CH(CH_3)_2$), 82.0 (m, $C(CF_3)_2$), 124.7 (q, $^1J_{CF}$ = 292.0, CF_3), 124.4, 124.9,126.6, 127.6, 128.0, 128.9 (*o*-, *m*-, *p*-Ph), 139.7 (*i*-Ph from N=C-Ph), resonances for the other two *ipso*-Ph carbons were not observed, 175.7 (C=N). $^{19}F\{^1H\}$ NMR (188 MHz, benzene-d_6, 298 K): δ −76.2 (s, 12F). $^{19}F\{^1H\}$ NMR (188 MHz, CD_2Cl_2, 298 K): δ −76.9 (s, 12F). Anal. Calcd for $C_{40}H_{38}F_{12}N_2O_4Ti$: C, 54.19; H, 4.32; N, 3.16. Found: C, 53.9; H, 4.5; N, 3.4.

Reaction of $\{ON^{Me,Ph}\}H$ with $TiCl_2(OiPr)_2$: Synthesis of $TiCl_2(OiPr)\{ON^{Me,Ph}\}$ (4). A solution of $Ti(OiPr)_4$ (24.0 mg, 84.4 μmol) in toluene (1 mL) was added to a solution of $TiCl_4$ (16.0 mg, 84.4 μmol) in toluene (1 mL). The mixture was stirred for 30 min at room temperature and then cooled to −30 °C. A solution of $\{ON^{Me,Ph}\}H$ (100 mg, 334 μmol, 2 equiv vs Ti) in hexane (2 mL), precooled at −30 °C, was then added dropwise to the previous solution. A precipitate immediately formed (65 mg, 37%). The solid was separated from solution by cannula, dried under vacuum, and recrystallized from dichloromethane at −30 °C to yield colorless crystals of **4**·*i*PrOH, which proved suitable for X-ray diffraction studies (30 mg, 17%). Anal. Calcd for $C_{18}H_{25}Cl_2F_6NO_3Ti$: C, 40.32; H, 4.70; N, 2.61. Found: C, 40.1; H, 4.6; N, 2.8. These crystals lose the coordinated 2-propanol molecule upon prolonged drying under vacuum to give **4**. ^1H NMR (300 MHz, CD_2Cl_2, 298 K): δ 1.15 (d, $^3J_{HH}$ = 5.8, 6H, $OCH(CH_3)_2$), 1.98 (s, 3H, CH_3), 3.21 (br s, 2H, CH_2), 4.54 (br m, 1H, $OCH(CH_3)_2$), 6.94 (br s, 2H, *o*-Ph), 7.24 (t, $^3J_{HH}$ = 7.6, 1H, *p*-Ph), 7.40 (t, $^3J_{HH}$ = 7.6, 2H, *m*-Ph). $^{13}C\{^1H\}$ NMR (75 MHz, CD_2Cl_2, 298 K): δ 24.0 ($CH(CH_3)_2$), 24.2 (CH_3), 39.6 (CH_2), 84.3 ($CH(CH_3)_2$), 121.7 (*o*-Ph), 125.9 (*p*-Ph), 129.0 (*m*-Ph), 147.7 (*i*-Ph), 174.6 (C=N). $^{19}F\{^1H\}$ NMR (188 MHz, CD_2Cl_2, 298 K): δ −77.6 (br s, 6F).

Reaction of $\{ON^{Ph,Ph}\}H$ with $TiCl_2(OiPr)_2$: Isolation of $TiCl(OiPr)\{ON^{Ph,Ph}\}_2$ (5) and $[TiCl_3\{ON^{Ph,Ph}\}\{ONH^{Ph,Ph}\}]$ (6). A solution of $Ti(OiPr)_4$ (10.0 mg, 35.2 μmol) in toluene (1 mL) was added to a solution of $TiCl_4$ (7.0 mg, 36.9 μmol) in toluene (1 mL). The mixture was stirred for 4 h at room temperature and then

(37) Similar catalytic behavior was observed upon using commercial MAO and DMAO (dried MAO from which most of the $AlMe_3$ has been removed).

(38) Zucchini, U.; Albizzati, E.; Giannini, U. *J. Organomet. Chem.* **1971**, *26*, 357.

cooled to −30 °C. A solution of {ON^{Ph,Ph}}H (50 mg, 138 μmol) in hexane (4 mL), precooled at −30 °C, was then added dropwise to the previous solution. The reaction mixture was gently warmed to room temperature overnight, after which time period colorless crystals appeared that proved suitable for X-ray diffraction studies (8.0 mg); the latter studies revealed that these crystals are a mixture of **5** and **6**. The ^{1}H and ^{19}F NMR spectra of this mixture showed many resonances that could not be assigned.

Reaction of $(CF_3)_2C(OH)CH_2C(=O)CH_3$ ({OO^{Me}}H) with $TiCl_2(OiPr)_2$: Synthesis of TiCl(O*i*Pr){OO^{Me}}$_2$. A solution of Ti(O*i*Pr)$_4$ (145 mg, 510 μmol) in toluene (3 mL) was added to a solution of $TiCl_4$ (97.0 mg, 511 μmol) in toluene (3 mL). The mixture was stirred for 30 min at room temperature and then cooled to −30 °C. A solution of $(CF_3)_2C(OH)CH_2C(=O)CH_3$ ({OO^{Me}}H) (445 mg, 1.99 mmol, 2 equiv vs Ti) in toluene (2 mL), precooled at −30 °C, was then added dropwise to the previous solution. The reaction mixture was gently warmed to room temperature overnight, volatiles were removed under vacuum, and the solid residue was washed with pentane (2 × 3 mL) and finally dried under vacuum to give TiCl(O*i*Pr){OO^{Me}}$_2$ as a white powder (280 mg, 48%). ^{1}H NMR (300 MHz, benzene-d_6, 298 K): δ 1.29 (d, $^3J_{HH}$ = 6.0, 6H, OCH(C*H*$_3$)$_2$), 1.49 (s, 6H, 2 CH$_3$), 2.75 (d, $^2J_{HH}$ = 16.0, 2H, C*H*H), 2.99 (br d, $^2J_{HH}$ = 16.0, 2H, CH*H*), 5.08 (hept, $^3J_{HH}$ = 6.0, 1H, OC*H*(CH$_3$)$_2$). ^{13}C{^{1}H} NMR (75 MHz, benzene-d_6, 298 K): δ 23.6 (CH(*C*H$_3$)$_2$), 31.5 (CH$_3$), 39.8 (CH$_2$), 87.6 (*C*H(CH$_3$)$_2$). ^{19}F{^{1}H} NMR (188 MHz, benzene-d_6, 298 K): δ −77.8 (br m, 6F), −77.5 (br s, 6F). Anal. Calcd for $C_6H_5Cl_2F_6O_2Ti$: C, 21.08; H, 1.47. Found: C, 21.5; H, 1.8.

Reaction of {ON^{Me,Ph}}H with Zr(CH$_2$Ph)$_4$: Synthesis of Zr(CH$_2$Ph)$_2${ON^{Me,Ph}}$_2$ (7a) and Zr(CH$_2$Ph){ON^{Me,Ph}}{ON$^{-Me,Ph}$} (9a). A solution of {ON^{Me,Ph}}H (200 mg, 668 μmol) in toluene (ca. 1 mL) precooled at −30 °C was added to a solution of Zr(CH$_2$Ph)$_4$ (152 mg, 334 μmol) in toluene at −30 °C. The mixture was kept standing in the freezer at −30 °C until some precipitate appeared. The supernatant solution was removed by pipet, and the solid residue was dried under vacuum to give **7a** as a yellow powder (182 mg, 29%). Suitable crystals for X-ray diffraction were grown from CD_2Cl_2 at −10 °C. ^{1}H NMR (500 MHz, CD_2Cl_2, 298 K): δ 1.81 (s, 6H, CH$_3$), 1.83 (s, 4H, CH$_2$), 1.92 (br s, 4H, C*H*$_2$Ph), 6.73−7.32 (m, 20H, Ph). ^{19}F{^{1}H} NMR (188 MHz, CD_2Cl_2, 298 K): δ −77.0 (s, 12F). ^{13}C{^{1}H} NMR (125 MHz, CD_2Cl_2, 298 K): δ 26.5 (CH$_3$), 36.8 (CH$_2$), 69.1 (*C*H$_2$−Ph), 178.6 (C=N); resonances for aromatic carbons were not assigned due to the presence of decomposition products (essentially **9a**, *vide infra*) that formed during data acquisition; resonances for quaternary carbons and CF$_3$ were not observed. Microanalysis of this compound was not possible due to its slow decomposition at room temperature in the solid state.

Decomposition of **7a** in toluene solution proceeded slowly at room temperature and was completed after one week, yielding **9a** as the major product (68% according to ^{1}H NMR). ^{1}H NMR (500 MHz, CD_2Cl_2, 298 K): δ (ppm) 1.80 (s, 3H, CH$_3$), 1.84 (s, 3H, CH$_3$), 2.00 (d, $^2J_{HH}$ =11.7, 1H, CH*H*-Ph), 2.17 (d, $^2J_{HH}$ =11.7, 1H, C*H*H-Ph), 2.66 (d, $^2J_{HH}$ = 16.2, 1H, C*H*H), 2.82 (d, $^2J_{HH}$ = 16.2, 1H, CH*H*), 4.56 (s, 1H, CH), from 6.53 to 7.45 (m, 15H, Ph). ^{19}F{^{1}H} NMR (188 MHz, CD_2Cl_2, 298 K): δ (ppm) −79.3 (br q, 3F), −78.9 (br q, 3F), −77.7 (br q, 3F), −77.5 (br q, 3F). ^{13}C{^{1}H} NMR (125 MHz, CD_2Cl_2, 298 K): δ 25.2 (CH$_3$), 25.9 (CH$_3$), 39.4 (CH$_2$), 66.6 (*C*H$_2$Ph), 94.4 (CH), 181.0 (C=N); for the same reasons as for **7a**, other resonances for **9a** could not be attributed or were not observed.

Reaction of {ON^{Ph,Ph}}H with Zr(CH$_2$Ph)$_4$: Synthesis of Zr(CH$_2$Ph)$_2${ON^{Ph,Ph}}$_2$ (7b) and Zr(CH$_2$Ph){ON^{Ph,Ph}}{ON$^{-Ph,Ph}$} (9b). NMR-scale reaction. In the glovebox, a Teflon-valved NMR tube was charged with pro-ligand {ON^{Ph,Ph}}H (21.0 mg, 58.0 μmol) and Zr(CH$_2$Ph)$_4$ (13.0 mg, 28.5 μmol). CD_2Cl_2 (ca. 0.5 mL) was vacuum-transferred in at low temperature, and the tube was kept at −20 °C for a few minutes until NMR was run immediately at room temperature. ^{1}H NMR spectroscopy showed quantitative and selective conversion of the reagents into **7b**. Repeated NMR data acquisitions after a short time period showed the appearance of resonances characteristic for the decomposition compound **9b** and toluene. Complete and selective decomposition of **7b** into **9b** was observed after 10 min. Preparation of X-ray suitable single crystals of **7b**: In the glovebox, a solution of {ON^{Ph,Ph}}H (40.0 mg, 110 μmol) in toluene (ca. 1 mL) precooled at −30 °C was added to a solution of Zr(CH$_2$Ph)$_4$ (25.0 mg, 54.9 μmol) in toluene (ca. 1 mL) at −30 °C. The mixture was kept standing in the freezer at −30 °C until crystals of **7b** appeared on the walls of the vial and were collected for X-ray data diffraction studies. Zr(CH$_2$Ph)$_2${ON^{Ph,Ph}}$_2$ (**7b**): ^{1}H NMR (300 MHz, CD_2Cl_2, 298 K): δ 2.05 (br s, 8H, CH$_2$), 6.75−7.26 (m, 30H, Ph). ^{19}F{^{1}H} NMR (188 MHz, CD_2Cl_2, 298 K): δ −76.5 (s, 12F). ^{19}F{^{1}H} NMR (188 MHz, toluene-d_8, 298 K): δ −80.9 (s, 12F). ^{13}C NMR and microanalysis of this compound were not possible due to its slow decomposition in solution as well as in the solid state. Zr(CH$_2$Ph){ON^{Ph,Ph}}{ON$^{-Ph,Ph}$} (**9b**): ^{1}H NMR (300 MHz, CD_2Cl_2, 298 K): δ 1.91 (d, $^2J_{HH}$ = 11.8, 1H, CH*H*-Ph), 2.21 (d, $^2J_{HH}$ = 11.8, 1H, C*H*H-Ph), 3.22 (d, $^2J_{HH}$ = 17.3, 1H, CH*H*), 3.32 (d, $^2J_{HH}$ = 17.3, 1H, C*H*H), 5.09 (s, 1H, CH), 6.63−7.26 (m, 25H, Ph). ^{1}H NMR (500 MHz, toluene-d_8, 298 K): δ 2.08 (d, $^2J_{HH}$ = 12.0, 1H, CH*H*Ph), 2.33 (d, $^2J_{HH}$ = 12.0, 1H, C*H*HPh), 2.98 (s, 2H, CH$_2$), 5.36 (s, 1H, CH), 6.71−7.13 (m, 25H, Ph). ^{19}F{^{1}H} NMR (188 MHz, CD_2Cl_2, 298 K): δ −79.2 (q, $^4J_{FF}$ = 9.2, 3F), −78.5 (q, $^4J_{FF}$ = 9.2, 3F), −78.3 (q, $^4J_{FF}$ = 10.3, 3F), −76.9 (q, $^4J_{FF}$ = 10.3, 3F). ^{19}F{^{1}H} NMR (188 MHz, toluene-d_8, 298 K): δ −83.8 (q, $^1J_{FF}$ = 9.4, 3F), −83.0 (2q overlapping, 6F), −81.5 (q, $^4J_{FF}$ = 9.4, 3F). Anal. Calcd for $C_{41}H_{30}F_{12}N_2O_2Zr$: C, 54.60; H, 3.35; N, 3.11. Found: C, 54.3; H, 3.4; N, 3.0.

NMR-Scale Reaction of {ON^{Ph,Bn}}H with Zr(CH$_2$Ph)$_4$: Synthesis of Zr(CH$_2$Ph){ON^{Ph,Bn}}{ON$^{-Ph,Bn}$} (9c). A Teflon-valved NMR tube was charged with {ON^{Ph,Bn}}H (20.0 mg, 53.3 μmol) and Zr(CH$_2$Ph)$_4$ (12.1 mg, 26.5 μmol), and CD_2Cl_2 (ca. 0.5 mL) was vacuum-transferred in at −78 °C. The tube was kept at low temperature until NMR was recorded at room temperature, which showed complete conversion of the reagents to **9c** (resonances for **7c** were not observed). ^{1}H NMR (300 MHz, CD_2Cl_2, 298 K): δ 1.71 (d, $^2J_{HH}$ = 10.8, 1H, Zr-CH*H*Ph), 2.05 (d, $^2J_{HH}$ = 10.8, 1H, Zr-C*H*HPh), 3.10 (d, $^2J_{HH}$ = 17.4, 1H, CH*H*C=N), 3.25 (d, $^2J_{HH}$ = 17.4, 1H, C*H*HC=N), 4.36 (d, $^2J_{HH}$ = 17.0, 1H, NCH*H*Ph), 4.60 (d, $^2J_{HH}$ = 17.0, 1H, NC*H*HPh), 4.60 (s, 1H, CH), 4.78 (d, $^2J_{HH}$ = 13.8, 1H, NCH*H*Ph), 5.17 (d, $^2J_{HH}$ = 13.8, 1H, NC*H*HPh), 6.81−7.45 (m, 25H, Ph). ^{19}F{^{1}H} NMR (188 MHz, CD_2Cl_2, 298 K): δ −78.4 (q, $^4J_{FF}$ = 9.4, 3F), −77.9 (2q overlapping, 6F), −77.2 (q, $^1J_{FF}$ = 9.4, 3F). Anal. Calcd for $C_{43}H_{34}F_{12}N_2O_2Zr$: C, 55.54; H, 3.69; N, 3.01. Found: C, 55.1; H, 3.9; N, 2.8.

Reaction of {ON^{Me,Ph}}H with Hf(CH$_2$Ph)$_4$: Synthesis of Hf(CH$_2$Ph)$_2${ON^{Me,Ph}}$_2$ (8a) and Hf(CH$_2$Ph){ON^{Me,Ph}}{ON$^{-Me,Ph}$} (10a). A Schlenk flask was charged with {ON^{Me,Ph}}H (101.5 mg, 0.34 mmol) and Hf(CH$_2$Ph)$_4$ (93.0 mg, 0.17 mmol), and toluene (ca. 5 mL) was vacuum-transferred in at −78 °C. The reaction mixture was stirred at room temperature for 1 h, over which time period some precipitate formed. The supernatant solution was removed by cannula, and the solid residue was dried under the vacuum, giving **8a** as an off-white solid (85 mg, 52%). The NMR tube was charged with this solid, and toluene-d_8 was vacuum-transferred in (ca. 0.5 mL). Crystals of **8a** suitable for X-ray diffraction studies were obtained by recrystallization from toluene. ^{1}H NMR (200 MHz, toluene-d_8, 298 K): δ 1.14 (s, 6H, CH$_3$), 1.43 (s, 4H, CH$_2$), 1.84 (br s, 4H, CH$_2$Ph), 6.48−7.10 (m, 20H, Ph). ^{19}F{^{1}H} NMR (188 MHz, toluene-d_8, 298 K): δ −76.5 (s, 12F). Anal. Calcd for $C_{38}H_{34}F_{12}HfN_2O_2$: C, 47.68; H, 3.58; N, 2.93. Found: C, 47.3; H, 3.4; N, 2.7. When a toluene-d_8 solution of **8a** was kept for 10 days at room temperature, the complex decomposed to form mainly **10a** (ca. 65%, as determined by ^{1}H NMR), as well as other minor (ca. 35%) unidentified secondary products. ^{1}H NMR

(200 MHz, CD_2Cl_2, 298 K): δ 1.48 (s, 3H, CH_3), 1.80 (d, $^2J_{HH}$ = 9.4, 1H, ^{CHHPh}), 1.98 (s, 3H, ^{CH_3}), 2.00 (d, $^2J_{HH}$ = 9.4, 1H, CHHPh), 2.67 (d, $^2J_{HH}$ = 16.5, 1H, CHH), 2.87 (d, $^2J_{HH}$ = 16.5, 1H, CHH), 4.51 (s, 1H, CH), 6.57−7.48 (m, 15H, Ph). $^{19}F\{^1H\}$ NMR (188 MHz, CD_2Cl_2, 298 K): δ −79.6 (q, $^4J_{FF}$ = 9.4, 3F), −79.1 (q, $^4J_{FF}$ = 9.4, 3F), −78.1 (q, $^4J_{FF}$ = 9.4, 3F), −77.6 (q, $^4J_{FF}$ = 9.4, 3F).

NMR-Scale Reaction of {ON^{Ph,Ph}}H with Hf(CH_2Ph)$_4$: Generation of Hf(CH_2Ph)$_2${ON^{Ph,Ph}}$_2$ (8b) and Hf(CH_2Ph)-{ON$^{-Ph,Ph}$}{ON$^{-Ph,Ph}$} (10b). A Teflon-valved NMR tube was charged with {ON^{Ph,Ph}}H (30.0 mg, 83.0 μmol) and Hf(CH_2Ph)$_4$ (22.5 mg, 41.4 μmol), and toluene-d_8 (ca. 0.5 mL) was vacuum-transferred in at −78 °C. The tube was kept at −78 °C until NMR spectroscopy was recorded at room temperature. ^1H NMR spectroscopy recorded after 1 min at this temperature revealed that all reagents were consumed and that transient **8b** quantitatively decomposed into **10b** and toluene. ^1H NMR (500 MHz, benzene-d_6, 298 K): δ 2.19 (d, $^2J_{HH}$ = 12.9, 1H, CH*H*Ph), 2.39 (d, $^2J_{HH}$ = 12.9, 1H, C*H*HPh), 3.04 (s, 2H, CH_2), 5.46 (s, 1H, CH), 6.78−7.27 (m, 25H, Ph). ^1H NMR (200 MHz, toluene-d_8, 298 K): δ 2.02 (d, $^2J_{HH}$ = 12.9, 1H, CH*H*Ph), 2.22 (d, $^2J_{HH}$ = 12.9, 1H, C*H*HPh), 2.94 (s, 2H, CH_2), 5.29 (s, 1H, CH), 6.71−7.13 (m, 25H, Ph). $^{19}F\{^1H\}$ NMR (188 MHz, toluene-d_8, 298 K): δ −79.0 (q, $^1J_{FF}$ = 9.4, 3F), −78.2 (2 q overl., $^1J_{FF}$ = 9.4, 6F), −76.5 (q, $^1J_{FF}$ = 9.4, 3F). $^{19}F\{^1H\}$ NMR (188 MHz, benzene-d_6, 298 K): δ −78.9 (q, $^4J_{FF}$ = 9.4, 3F), −78.2 (q, $^4J_{FF}$ = 9.4, 3F), −78.1 (q, $^4J_{FF}$ = 9.4, 3F), −76.5 (q,$^4J_{FF}$ = 9.4, 3F).

Reaction of {ON^{Me,ArF}}H with Zr(CH_2Ph)$_4$: Synthesis of Zr(CH_2Ph)$_2${ON^{Me,ArF}}$_2$ (7d) and Zr{ON^{Me,ArF}}$_2${ON$^{-Me,ArF}$} (11). A Teflon-valved NMR tube was charged with {ON^{Me,ArF}}H (68.3 mg, 175.5 μmol) and Zr(CH_2Ph)$_4$ (40.0 mg, 87.8 μmol), and toluene-d_8 (ca. 0.5 mL) was vacuum-transferred in at −78 °C. The tube was kept for 3−4 h at −30 °C, and afterward NMR spectroscopy was recorded at room temperature. The formation of **7d** proceeded in ca. 80% yield according to ^1H NMR. Green-yellow crystals of **7d** suitable for X-ray diffraction studies were obtained by cooling the solution at −30 °C for 20 h (10 mg, 11% yield). ^1H NMR (500 MHz, toluene-d_8, 298 K): δ 1.19 (s, 6H, CH_3), 2.38 (s, 4H, C*H*$_2$Ph), 2.74 (s, 4H, CH_2), 6.86−7.09 (m, 10H, Ph). $^{19}F\{^1H\}$ NMR (188 MHz, toluene-d_8, 298 K): δ −167.2 (m, 4F, *m*-F), −162.7 (t, 2F, *p*-F), −151.9 (br s, 4F, *o*-F), −82.3 (s, 12F, CF_3). Due to the instability of **7d** at room temperature in toluene solution, ^{13}C NMR and HETCOR spectra were not recorded. The toluene solution of **7d** was kept in the glovebox at ambient temperature for one day, after which time period pale-yellow crystals of **11** suitable for X-ray diffraction studies were recovered (36.3 mg, 33% yield). ^1H NMR (500 MHz, benzene-d_6, 298 K): δ 1.02 (s, 3H, CH_3), 1.04 (s, 6H, CH_3), 3.16 (s, 4H, CH_2), 4.82 (s, 1H, CH). $^{13}C\{^1H\}$ NMR (125 MHz, benzene-d_6, 298 K): δ 22.3 (CH_3), 26.0 (CH_3), 39.8 (CH_2), 81.3 ($C(CF_3)_2$), 99.3 (CH), 150.0 (CH═*C*(CH_3)N), 193.3 (C═N); the remaining resonances were not observed by HMQC and HMBC methods. $^{19}F\{^1H\}$ NMR (188 MHz, benzene-d_6, 298 K): δ −165.5 (m, 2F, *p*-F), −161.9 (m, 5F, *m*- and *p*-F), −155.9 (m, 2F, *m*-F), −149.2−−146.7 (br m, 6F, *o*-F), −78.0 (s, 6F, CF_3), −77.5 (s, 12F, CF_3). Anal. Calcd for $C_{36}H_{14}F_{33}N_3O_3Zr$: C, 34.46; H, 1.12; N, 3.35. Found: C, 35.10; H, 1.50; N, 3.3.

Synthesis of ZrCl$_2${ON^{Me,Ph}}$_2$ (12a). A slurry of $ZrCl_4$ (192 mg, 0.824 mmol) in toluene (30 mL) was cooled at −78 °C, and *n*BuLi (0.66 mL of a 2.5 M solution in hexanes, 1.65 mmol, 2 equiv) was added dropwise. After 25 min of stirring at room temperature, the light brown solution was cooled at −50 °C, and a solution of {ON^{Me,Ph}}H (496 mg, 1.66 mmol) in toluene (10 mL) was added dropwise. The reaction mixture was stirred at room temperature overnight and then filtered. The clear filtrate was concentrated under vacuum, and the resulting sticky residue was washed with dry hexane (ca. 5 mL) and dried under vacuum to give **12a** as a white powder (245 mg, 39%). Anal. Calcd for $C_{24}H_{20}Cl_2F_{12}N_2O_2Zr$: C, 38.00; H, 2.66; N, 3.69. Found: C, 38.1; H, 2.8; N, 3.6. NMR revealed that this product is a 70:30 mixture of two isomers: the major one is C_{2v}-symmetric and the minor one is C_1-symmetric. Heating of this mixture at 70 °C for 48 h in benzene-d_6 led to a 77:23 mixture of C_{2v}- and C_1-**12b**, as monitored by ^1H NMR. When this mixture of isomers was extracted in hot hexanes, the insoluble powder left after filtration was shown to be exclusively the C_1-symmetric isomer. C_{2v}-**12a**: ^1H NMR (500 MHz, benzene-d_6, 298 K): δ (ppm) 1.09 (s, 6H, CH_3), 3.03 (s, 4H, CH_2), 6.82 (d, $^3J_{HH}$ = 7.6 Hz, 4H, *o*-Ph), 6.95 (t, $^3J_{HH}$ = 7.6 Hz, 2H, *p*-Ph), 7.07 (t, $^3J_{HH}$ = 7.6 Hz, 4H, *m*-Ph). $^{13}C\{^1H\}$ NMR (125 MHz, benzene-d_6, 298 K): δ 25.1 (CH_3), 40.0 (CH_2), 81 (m, $C(CF_3)_2$), 123.1 (*o*-Ph), 123.6 (q, $^1J_{CF}$ = 303.7, CF_3), 127.1 (*p*-Ph), 129.4 (*m*-Ph), 146.6 (*i*-Ph), 183.2 (C═N). $^{19}F\{^1H\}$ NMR (188 MHz, benzene-d_6, 298 K): δ −76.5 (s, 12F). C_1-**12a**: ^1H NMR (500 MHz, benzene-d_6, 298 K): δ 1.15 (s, 3H, CH_3), 1.53 (s, 3H, CH_3), 2.70 (d, $^2J_{HH}$ = 15.0, 1H, C*H*H), 3.17 (d, $^2J_{HH}$ = 15.8, 1H, CH*H*), 3.55 (d, $^2J_{HH}$ = 15.0, 1H, C*H*H), 4.27 (d, $^2J_{HH}$ = 15.8, 1H, CH*H*), 5.37 (br d, $^3J_{HH}$ = 7.2, 1H, *o*-Ph), 6.63−7.25 (m, 8H, Ph), 8.19 (br d, $^3J_{HH}$ = 7.5, 1H, *o*-Ph). $^{19}F\{^1H\}$ NMR (188 MHz, benzene-d_6, 298 K): δ −79.1 (br s, 3F), −77.8 (br s, 3F), −75.5 (q, $^1J_{FF}$ = 10.3, 3F), −75.1 (br s, 3F). $^{13}C\{^1H\}$ NMR (125 MHz, benzene-d_6, 298 K): δ 25.6 (CH_3), 26.6 (CH_3), 39.0 (CH_2), 40.3 (CH_2), 80.5 (m, $C(CF_3)_2$), 81.4 (m, $C(CF_3)_2$), 120.7 (*o*-Ph), 123.0 (*o*-Ph), 124.7 (q, $^1J_{CF}$ = 297.1, CF_3), 124.8 (q, $^1J_{CF}$ = 312.4, CF_3), 125.4 (*o*-Ph), 125.9 (*p*-Ph), 126.0 (*o*-Ph), 126.4 (*p*-Ph), 129.0 (*m*-Ph), 129.3 (2 *m*-Ph), 130.0 (*m*-Ph), 148.4 (*i*-Ph), 149.5 (*i*-Ph), 177.4 (*C*═N), 182.8 (C═N).

Synthesis of ZrCl$_2${ON^{Ph,Ph}}$_2$ (12b). This compound was prepared following a procedure similar to the one described above for **12a**, starting from $ZrCl_4$ (161 mg, 0.691 mmol) and {ON^{Ph,Ph}}H (500 mg, 1.384 mmol). Compound **12b** was obtained as a white powder (170 mg, 28%), which proved to be a 30:70 mixture of a C_{2v}-symmetric and a C_1-symmetric isomer. Heating of this mixture at 70 °C for 2.5 days in benzene-d_6 led to the complete and selective transformation to C_{2v}-**12b**, as monitored by ^1H NMR. Extraction of the C_{2v}/C_1-mixture with hot hexanes left a residue that proved to be analytically pure C_1-**12b**. C_{2v}-**12b**: ^1H NMR (300 MHz, benzene-d_6, 298 K): δ 3.66 (s, 4H, CH_2), 6.46−7.42 (m, 20H, Ph). $^{19}F\{^1H\}$ NMR (188 MHz, benzene-d_6, 298 K): δ −76.5 (s, 12F). C_1-**12b**: ^1H NMR (500 MHz, benzene-d_6, 298 K): δ 3.42 (d, $^2J_{HH}$ = 15.5, 1H, C*H*H), 3.94 (d, $^2J_{HH}$ = 17.0, 1H, CH*H*), 4.32 (d, $^2J_{HH}$ = 15.5, 1H, C*H*H), 5.01 (d, $^2J_{HH}$ = 17.0, 1H, CH*H*), 5.44 (br d, 1H, *o*-Ph), 6.3 (br t, 1H, *m*-Ph), 6.54 (m, 1H, Ph), 6.60−6.68 (m, 10H, Ph), 6.84 (t, $^3J_{HH}$ = 7.9, 2H, Ph), 7.21 (br t, 1H, *m*-Ph), 7.46 (m, 3H, Ph), 8.77 (br d, 1H, *o*-Ph). $^{19}F\{^1H\}$ NMR (188 MHz, benzene-d_6, 298 K): δ (ppm) −78.8 (br m, 3F), −77.7 (br m, 3F), −74.8 (2 m overl., 6F). Anal. Calcd for $C_{34}H_{24}Cl_2F_{12}N_2O_2Zr$: C, 46.26; H, 2.74; N, 3.17. Found: C, 46.5; H, 2.9; N, 3.3.

Synthesis of ZrCl$_2${ON^{Me,ArF}}$_2$ (12c). To a solution of {ON^{Me,ArF}}H (0.70 g, 1.80 mmol) in Et_2O (30 mL) kept at −78 °C was added dropwise *n*BuLi (0.72 mL of a 2.5 M solution in hexanes, 1.80 mmol). The reaction mixture was stirred for 3 h at −78 °C and then allowed to warm to room temperature over 1 h. Volatiles were removed under vacuum, and solid $ZrCl_4$ (0.21 g, 0.90 mmol) was added to the mixture in the glovebox. Et_2O (30 mL) was vacuum-transferred to the reaction mixture, and the latter was stirred for 12 h at room temperature. Volatiles were removed under vacuum, and dichloromethane (30 mL) was vacuum-transferred onto the solid residue. The resulting solution was filtered off, the pale pink solution was concentrated to ca. 5−7 mL, hexane (5 mL) was added, and the solution was left at −30 °C. After 10 h, a pink microcrystalline solid precipitated out. This was separated and dried under vacuum to give **12c** as a white solid (0.100 g, 12%). This compound featured extremely poor solubility in all common solvents, which hampered characterization by NMR. Anal. Calcd for $C_{24}H_{10}Cl_2F_{22}N_2O_2Zr$: C, 30.72; H, 1.07; N, 2.99. Found: C, 30.5; H, 1.0; N, 3.1.

Reaction of {ON^{R1,R2}}H with Na: Synthesis of {ON^{R1,R2}}Na. {ON^{Ph,Ph}}Na: In a typical experiment, in the glovebox, a Schlenk flask was charged with {ON^{Ph,Ph}}H (514 mg, 1.42 mmol) and Na powder (32.7 mg, 1.42 mmol). Dry THF (ca. 10 mL) was vacuum-transferred in at −78 °C, and the mixture was stirred overnight at room temperature. Volatiles were removed under vacuum, and the solid residue was washed with hexane (ca. 5 mL) and dried under vacuum to give {ON^{Ph,Ph}}Na as a white powder (355 mg, 65%). ^{1}H NMR (200 MHz, benzene-d_6, 298 K): δ 3.21 (s, 2H, CH_2), 6.78−7.05 (m, 10H, Ph). ^{19}F{^{1}H} NMR (188 MHz, benzene-d_6, 298 K): δ −78.5 (s, 6F, CF_3). Anal. Calcd for $C_{17}H_{12}F_6NNaO$: C, 53.27; H, 3.16; N, 3.65. Found: C, 53.4; H, 3.3; N, 3.6. Synthesis of {ON^{Me,Ph}}Na: This compound was prepared following a similar procedure to the one described above for {ON^{Ph,Ph}}Na, starting from {ON^{Me,Ph}}H (500 mg, 1.67 mmol) and Na powder (38.5 mg, 1.67 mmol). {ON^{Me,Ph}}Na was obtained as a white powder (370 mg, 69%). ^{1}H NMR (500 MHz, THF-d_8, 298 K): δ 1.79 (s, 3H, CH_3), 2.64 (s, 2H, CH_2), 6.60 (br d, 2H, *o*-Ph), 7.00 (t, $^3J_{HH}$ = 7.8, 1H, *p*-Ph), 7.22 (m, 2H, *m*-Ph). ^{19}F{^{1}H} NMR (188 MHz, THF-d_8, 298 K): δ −81.0 (s, 6F, CF_3). Anal. Calcd for $C_{12}H_{10}F_6NNaO$: C, 44.87; H, 3.14; N, 4.36. Found: C, 45.0; H, 3.2; N, 4.2.

Reaction of {ON^{R1,R2}}H with KH: Synthesis of {ON^{R1,R2}}K and {ON$^{-R1,R2}$}K$_2$. (a) {ON^{Me,ArF}}K. This compound was prepared following a similar procedure to the one described above for {ON^{Ph,Ph}}Na, starting from {ON^{Me,ArF}}H (120 mg, 0.308 mmol) and KH (13.0 mg, 0.324 mmol). {ON^{Me,Ph}}K was obtained as a white powder (80 mg, 61%). ^{1}H NMR (500 MHz, THF-d_8, 298 K): δ 2.04 (s, 3H, CH_3), 2.81 (s, 2H, CH_2). ^{19}F{^{1}H} NMR (188 MHz, THF-d_8, 298 K): δ −167.4 (t, $^3J_{CF}$ = 20.7, 1F, *p*-CF), −166.5 (t, $^3J_{CF}$ = 20.7, 2F, *m*-CF), −154.7 (d, $^3J_{CF}$ = 20.7, 2F, *o*-CF), −79.2 (s, 6F, CF_3).

(b) {ON^{Me,Ph}}K. This compound was prepared following a similar procedure to the one described above for {ON^{Ph,Ph}}Na, starting from {ON^{Me,Ph}}H (99.0 mg, 0.331 mmol) and KH (13.2 mg, 0.331 mmol). The reaction time was 1 h, and {ON^{Me,Ph}}K was obtained as an off-white powder (72 mg, 65%). ^{1}H NMR (500 MHz, THF-d_8, 298 K): δ 1.82 (s, 3H, CH_3), 2.65 (s, 2H, CH_2), 6.61 (d, $^3J_{HH}$ = 7.9, 2H, *o*-Ph), 6.96 (t, $^3J_{HH}$ = 7.9, 1H, *p*-Ph), 7.21 (t, $^3J_{HH}$ = 7.9, 2H, *m*-Ph). ^{19}F{^{1}H} NMR (188 MHz, THF-d_8, 298 K): δ −78.8 (s, 6F, CF_3).

(c) {ON$^{-Me,Ph}$}K$_2$. This compound was prepared as described above, starting from {ON^{Me,Ph}}H (100 mg, 0.334 mmol) and KH (26.7 mg, 0.667 mmol) and leaving the reaction overnight. {ON$^{-Me,Ph}$}K$_2$ was obtained as an off-white powder (86 mg, 69%). ^{1}H NMR (500 MHz, THF-d_8, 298 K): δ 1.68 (s, 3H, CH_3), 4.87 (s, 1H, =CH), 6.63 (d, $^3J_{HH}$ = 7.6, 2H, *o*-Ph), 6.85 (t, $^3J_{HH}$ = 7.6, 1H, *p*-Ph), 7.16 (t, $^3J_{HH}$ = 7.6, 2H, *m*-Ph). ^{19}F{^{1}H} NMR (188 MHz, THF-d_8, 298 K): δ −75.6 (s, 6F, CF_3). Anal. Calcd for $C_{12}H_9F_6K_2NO$: C, 38.39; H, 2.42; N, 3.73. Found: C, 38.1; H, 2.5; N, 3.7.

Crystal Structure Determinations. As stated above, suitable crystals for X-ray diffraction analysis of **1**, **3a**, **4**, **5**, **6**, **7a**, **7b**, **7d**, **8a**, and **11** were obtained by recrystallization of purified products or in the course of synthetic reactions. Diffraction data were collected at 100 K using a Bruker APEX CCD diffractometer with graphite-monochromated Mo Kα radiation (λ = 0.71073 Å). A combination of ω and ϕ scans was carried out to obtain at least a unique data set. The crystal structures were solved by means of the Patterson method; remaining atoms were located from difference Fourier synthesis followed by full-matrix least-squares refinement based on F^2 (programs SHELXS-97 and SHELXL-97).[39] Many hydrogen atoms could be found from the Fourier difference analysis. Carbon-bound hydrogen atoms were placed at calculated positions and forced to ride on the attached atom. The hydrogen atom contributions were calculated but not refined. All non-hydrogen atoms were refined with anisotropic displacement parameters. The locations of the largest peaks in the final difference Fourier map calculation as well as the magnitude of the residual electron densities were of no chemical significance. In **5**, one trifluoromethyl group was found to be disordered and accordingly modeled. Crystals of **6** and **11** were found to contain lattice disordered solvent molecules (toluene), which could not be sufficiently modeled in the refinement cycles. These molecules were removed using the SQUEEZE procedure[40] implemented in the PLATON package.[41] Crystal data and details of data collection and structure refinement for the different compounds are given in Table 1. Crystallographic data are also available as cif files (see the Supporting Information).

Ethylene Polymerization. Polymerization experiments (Table 2) were performed in a 320 mL high-pressure glass reactor equipped with a mechanical stirrer and externally heated with a double mantle with a circulating water bath as desired. The reactor was filled with toluene (50 mL) and MAO (30 wt % solution in toluene, 3.0−3.8 mL, 1100−1500 equiv) or Al(*i*Bu)$_3$ (0.5−3.2 mL, 40−100 equiv) and [Ph$_3$C][B(C$_6$F$_5$)$_4$] (25−60 mg, 2−3 equiv) and pressurized at 7−8 atm of ethylene (Air Liquide, 99.99%). The reactor was thermally equilibrated at the desired temperature for 1 h. Ethylene pressure was decreased to 1 atm, and the catalyst precursor (12−32 μmol) in toluene (ca. 1 mL) was added by syringe. The ethylene pressure was immediately increased to 7−8 atm, and the solution was stirred for the desired time. Ethylene consumption was monitored using an electronic manometer connected to a secondary 100 mL ethylene tank, which feeds the reactor by maintaining constant the total pressure. The polymerization was stopped by venting of the vessel and quenching with a 10% HCl solution in methanol (ca. 3 mL). The polymer was precipitated in methanol (ca. 200 mL), and 35% aqueous HCl (ca. 1 mL) was added to dissolve possible catalyst residues. The polymer was collected by filtration, washed with methanol (ca. 200 mL), and dried under vacuum overnight.

Melting temperatures of PE samples were determined on a Perkin-Elmer Pyris 1 differential scanning calorimeter (10 °C/min, nitrogen flow, first pass). Gel permeation chromatography (GPC) analyses were performed at the University of Chicago on a Polymer Laboratories PL-GPC 220 instrument using 1,2,4-trichlorobenzene as solvent (stabilized with 125 ppm BHT) at 150 °C. A set of three PLgel 10 μm Mixed-B or Mixed-B LS columns was used. Samples were prepared at 160 °C and filtered through 2 or 5 μm stainless steel frits prior to injection. Molecular weights were determined versus polystyrene standards and are reported relative to polyethylene standards, as calculated by the universal calibration method using Mark−Houwink parameters (K = 17.5 × 10^{-5}, α = 0.670 for polystyrene; K = 40.6 × 10^{-5}, α = 0.725 for polyethylene).

Acknowledgment. This work was financially supported in part by Agence Nationale de la Recherche (grant ANR-06-BLAN-0213) and Total Co. (Ph.D. grant to N.M.; postdoctoral fellowship to E.K.). We are most grateful to Prof. R. F. Jordan (Univ. Chicago) for HT-GPC analyses. J.F.C. thanks the Institut Universitaire de France for a Junior IUF fellowship (2005−2009).

Supporting Information Available: Crystallographic data for **1**, **3a**, **4**, **5**, **6**, **7a**, **7b**, **7d**, **8a**, and **11** as CIF files; representative GPC traces and DSC profiles of PEs prepared. This material is available free of charge via the Internet at http://pubs.acs.org.

OM8009409

(39) (a) Sheldrick, G. M. *SHELXS-97*, Program for the Determination of Crystal Structures; University of Goettingen: Germany, 1997. (b) Sheldrick, G. M. *SHELXL-97*, Program for the Refinement of Crystal Structures; University of Goettingen: Germany, 1997.

(40) van der Sluis, P.; Spek, A. L. *Acta Crystallogr.* **1990**, *A46*, 194.
(41) Spek, A. L. *Acta Crystallogr.* **1990**, *A46*, C-34.